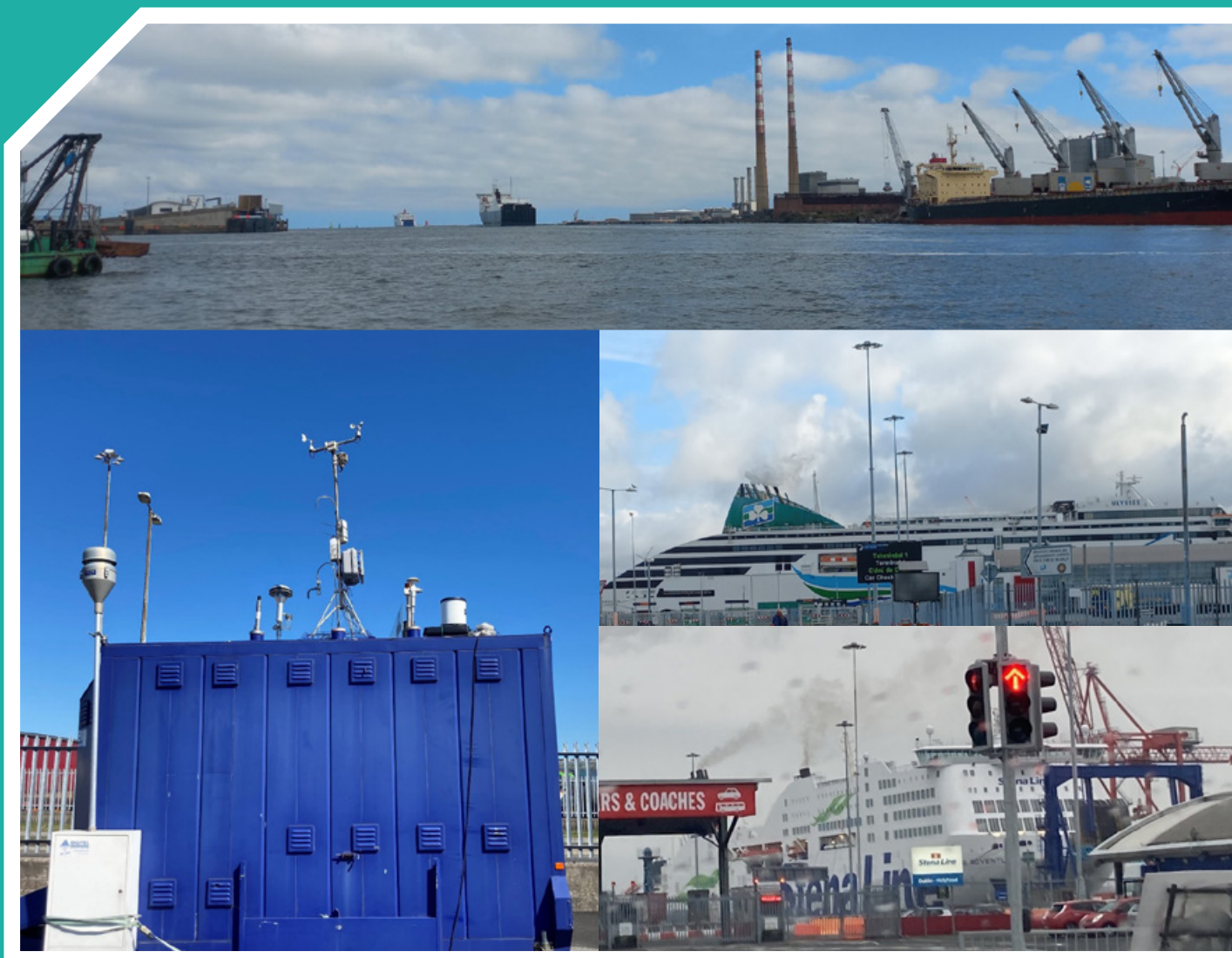


Source Apportionment of Air Pollution in the Dublin Port Area (PortAIR)

Authors: Kirsten Fossum, Niall O'Sullivan, Srishti Jain, Lu Lei, Chunshui Lin, Darius Ceburnis, Stig Hellebust, Colin O'Dowd, Jurgita Ovadnevaite and John Wenger

Lead organisation: University College Cork and University of Galway



Environmental Protection Agency

The EPA is responsible for protecting and improving the environment as a valuable asset for the people of Ireland. We are committed to protecting people and the environment from the harmful effects of radiation and pollution.

The work of the EPA can be divided into three main areas:

Regulation: Implementing regulation and environmental compliance systems to deliver good environmental outcomes and target those who don't comply.

Knowledge: Providing high quality, targeted and timely environmental data, information and assessment to inform decision making.

Advocacy: Working with others to advocate for a clean, productive and well protected environment and for sustainable environmental practices.

Our Responsibilities Include:

Licensing

- > Large-scale industrial, waste and petrol storage activities;
- > Urban waste water discharges;
- > The contained use and controlled release of Genetically Modified Organisms;
- > Sources of ionising radiation;
- > Greenhouse gas emissions from industry and aviation through the EU Emissions Trading Scheme.

National Environmental Enforcement

- > Audit and inspection of EPA licensed facilities;
- > Drive the implementation of best practice in regulated activities and facilities;
- > Oversee local authority responsibilities for environmental protection;
- > Regulate the quality of public drinking water and enforce urban waste water discharge authorisations;
- > Assess and report on public and private drinking water quality;
- > Coordinate a network of public service organisations to support action against environmental crime;
- > Prosecute those who flout environmental law and damage the environment.

Waste Management and Chemicals in the Environment

- > Implement and enforce waste regulations including national enforcement issues;
- > Prepare and publish national waste statistics and the National Hazardous Waste Management Plan;
- > Develop and implement the National Waste Prevention Programme;
- > Implement and report on legislation on the control of chemicals in the environment.

Water Management

- > Engage with national and regional governance and operational structures to implement the Water Framework Directive;
- > Monitor, assess and report on the quality of rivers, lakes, transitional and coastal waters, bathing waters and groundwaters, and measurement of water levels and river flows.

Climate Science & Climate Change

- > Publish Ireland's greenhouse gas emission inventories and projections;

- > Provide the Secretariat to the Climate Change Advisory Council and support to the National Dialogue on Climate Action;
- > Support National, EU and UN Climate Science and Policy development activities.

Environmental Monitoring & Assessment

- > Design and implement national environmental monitoring systems: technology, data management, analysis and forecasting;
- > Produce the State of Ireland's Environment and Indicator Reports;
- > Monitor air quality and implement the EU Clean Air for Europe Directive, the Convention on Long Range Transboundary Air Pollution, and the National Emissions Ceiling Directive;
- > Oversee the implementation of the Environmental Noise Directive;
- > Assess the impact of proposed plans and programmes on the Irish environment.

Environmental Research and Development

- > Coordinate and fund national environmental research activity to identify pressures, inform policy and provide solutions;
- > Collaborate with national and EU environmental research activity.

Radiological Protection

- > Monitoring radiation levels and assess public exposure to ionising radiation and electromagnetic fields;
- > Assist in developing national plans for emergencies arising from nuclear accidents;
- > Monitor developments abroad relating to nuclear installations and radiological safety;
- > Provide, or oversee the provision of, specialist radiation protection services.

Guidance, Awareness Raising, and Accessible Information

- > Provide independent evidence-based reporting, advice and guidance to Government, industry and the public on environmental and radiological protection topics;
- > Promote the link between health and wellbeing, the economy and a clean environment;
- > Promote environmental awareness including supporting behaviours for resource efficiency and climate transition;
- > Promote radon testing in homes and workplaces and encourage remediation where necessary.

Partnership and Networking

- > Work with international and national agencies, regional and local authorities, non-governmental organisations, representative bodies and government departments to deliver environmental and radiological protection, research coordination and science-based decision making.

Management and Structure of the EPA

The EPA is managed by a full time Board, consisting of a Director General and five Directors. The work is carried out across five Offices:

1. Office of Environmental Sustainability
2. Office of Environmental Enforcement
3. Office of Evidence and Assessment
4. Office of Radiation Protection and Environmental Monitoring
5. Office of Communications and Corporate Services

The EPA is assisted by advisory committees who meet regularly to discuss issues of concern and provide advice to the Board.

Source Apportionment of Air Pollution in the Dublin Port Area (PortAIR)

Authors: Kirsten Fossum, Niall O’Sullivan, Srishti Jain, Lu Lei, Chunshui Lin, Darius Ceburnis, Stig Hellebust, Colin O’Dowd, Jurgita Ovadnevaite and John Wenger

Lead organisation: University College Cork and University of Galway

What did this research aim to address?

Dublin Port is Ireland’s largest freight and passenger port, handling a significant portion of the country’s international trade and playing a crucial role in the national and regional economies. While the port brings significant economic and social benefits, the emissions from ships and other port-related activities contribute to climate change and air pollution, affecting the health of citizens and the environment. The principal objective of the PortAIR project was to conduct the first detailed study of the impact of ships and other pollution sources on air quality in the Dublin Port area. This was achieved through a combined measurement–analysis approach involving continuous monitoring of air pollution and the chemical composition of particulate matter (PM) throughout 2022, a multi-instrument intensive field campaign conducted during the height of shipping activity, and advanced source apportionment modelling methods. This innovative approach delivered new results on air pollution sources to enable Dublin Port Company and other stakeholders (Dublin City Council, the EPA, government departments) to develop targeted strategies for reducing emissions in Dublin Port.

What did this research find?

Hundreds of ship plumes were observed as discrete pollution events and categorised into two main types using known chemical markers. The first plume type contained PM dominated by sulfate, attributed to ships using high-sulfur heavy fuel oil and fitted with a scrubber system to reduce SO₂ emissions. The second plume type contained PM dominated by organic species, attributed to ships using low-sulfur marine fuels. Ship emissions were at their highest while manoeuvring in and out of the berth, while smaller amounts of pollutants were emitted over a longer timescale when vessels were docked. The main sources of PM_{2.5} at the PortAIR site during 2022 were regional background (56%) and ship emissions (21%), with vehicles and home heating largely accounting for the remainder. Ship plumes were the main source of SO₂ and contributed significantly to both submicron particle number concentration and NO_x. While the prevailing westerly winds generally carried port-based emissions towards the Irish Sea, data obtained from an air sensor network showed that port emissions caused an increase of up to 6% in PM_{2.5} in parts of the city adjacent to the port.

How can the research findings be used?

The planned expansion of Dublin Port will lead to greater ship emissions, and it is therefore recommended that measures to reduce air pollution are introduced. The provision of shore-side electricity to vessels at berth has already been identified as a good way of reducing emissions and is specifically mentioned in the Dublin Port Masterplan. The introduction of a designated Emission Control Area for the North-East Atlantic region would control NO_x emissions from ships and further reduce SO₂ and particulate matter. The use of battery-powered ferries and small vessels are also worthy of consideration, along with switching to renewable or low-carbon fuels for ships. However, further research into the pros and cons of these approaches is required. This research clearly demonstrated the value of sophisticated research-grade instruments for online continuous monitoring of PM. It is recommended that future field measurement campaigns also utilise instruments for monitoring fine and ultrafine particle number concentration, as well as online elemental analysis to provide a more complete understanding of the sources and health impacts of ambient PM.

EPA RESEARCH PROGRAMME 2021–2030

Source Apportionment of Air Pollution in the Dublin Port Area (PortAIR)

(2020-CCRP-LS.6)

EPA Research Report

Prepared for the Environmental Protection Agency

by

University College Cork and University of Galway

Authors:

**Kirsten Fossum, Niall O’Sullivan, Srishti Jain, Lu Lei, Chunshui Lin, Darius Ceburnis,
Stig Hellebust, Colin O’Dowd, Jurgita Ovadnevaite and John Wenger**

ENVIRONMENTAL PROTECTION AGENCY

An Ghníomhaireacht um Chaomhnú Comhshaoil
PO Box 3000, Johnstown Castle, Co. Wexford, Ireland

Telephone: +353 53 916 0600 Fax: +353 53 916 0699

Email: info@epa.ie Website: www.epa.ie

ACKNOWLEDGEMENTS

This report is published as part of the EPA Research Programme 2021–2030. The EPA Research Programme is a Government of Ireland initiative funded by the Department of Climate, Energy and the Environment. It is administered by the Environmental Protection Agency, which has the statutory function of co-ordinating and promoting environmental research.

The authors would like to acknowledge the members of the project steering committee, namely Gary Fuller (Imperial College London), Eamon McElroy (Dublin Port Company), Sarah Boylan and Patrick Kenny (Environmental Protection Agency), Micheál Young (Department of Climate, Energy and the Environment) and Maurice Harnett (Department of Transport); also John McEntagart, Anna Shore and Oonagh Monahan, Research Project Managers on behalf of the EPA.

The authors would like to thank the following collaborators for their valuable contributions to the project: Anja Tremper and David Green (Imperial College London) for loan of the Xact instrument; Lila Diapouli, Stefanos Papagiannis and Kostas Eleftheriadis (The Institute of Nuclear & Radiological Sciences and Technology, Energy & Safety, National Centre of Scientific Research “Demokritos”) for elemental analysis of offline samples to obtain elemental composition as well as organic and elemental carbon; and Steigvilė Byčėnienė and Vadimas Dudoitis (SRI Center for Physical Sciences and Technology, Lithuania) for loan of the PM₁ Q-ACSM instrument.

Finally, the authors would like to thank Eamon McElroy, Ken Rooney, John Dungan and colleagues in Dublin Port Company for enabling site access and providing valuable support and port-related information; Stena Line, especially Eamon Fortune, for access to facilities and the sampling site; and numerous representatives from the shipping companies that provided details of ship fuel use.

DISCLAIMER

Although every effort has been made to ensure the accuracy of the material contained in this publication, complete accuracy cannot be guaranteed. The Environmental Protection Agency, the authors and the steering committee members do not accept any responsibility whatsoever for loss or damage occasioned, or claimed to have been occasioned, in part or in full, as a consequence of any person acting, or refraining from acting, as a result of a matter contained in this publication. Any opinions, findings or recommendations expressed in this report are those of the authors and do not reflect a position or recommendation of the EPA. All or part of this publication may be reproduced without further permission, provided the source is acknowledged.

This report is based on research carried out/data from 1 March 2021 to 29 February 2024. More recent data may have become available since the research was completed.

The EPA Research Programme addresses the need for research in Ireland to inform policymakers and other stakeholders on a range of questions in relation to environmental protection. These reports are intended as contributions to the necessary debate on the protection of the environment.

EPA RESEARCH PROGRAMME 2021–2030
Published by the Environmental Protection Agency, Ireland

ISBN: 978-1-80009-314-0

October 2025

Price: Free

Online version

Project Partners

Professor John Wenger

School of Chemistry and Environmental
Research Institute
University College Cork
Cork
Ireland
Email: j.wenger@ucc.ie

Dr Stig Hellebust

School of Chemistry and Environmental
Research Institute
University College Cork
Cork
Ireland
Email: s.hellebust@ucc.ie

Professor Jurgita Ovadnevaite

School of Natural Sciences, Physics
The Ryan Institute's Centre for Climate and Air
Pollution Studies
University of Galway
Galway
Ireland
Email: jurgita.ovadnevaite@universityofgalway.ie

Professor Colin O'Dowd

School of Natural Sciences, Physics
The Ryan Institute's Centre for Climate and Air
Pollution Studies
University of Galway
Galway
Ireland
Email: colin.odowd@universityofgalway.ie

Contents

| | |
|--|-------------|
| Acknowledgements | ii |
| Disclaimer | ii |
| Project Partners | iii |
| List of Figures | vi |
| List of Tables | viii |
| Executive Summary | ix |
| 1 Introduction | 1 |
| 1.1 Background | 1 |
| 1.2 Air Pollution in Port Areas | 2 |
| 1.3 The PortAIR Project | 3 |
| 2 Methods | 4 |
| 2.1 Field Measurements | 4 |
| 2.2 Instrumentation | 5 |
| 2.3 Source Apportionment | 8 |
| 2.4 Reconstruction of PM _{2.5} Mass Concentration | 9 |
| 3 Results and Discussion | 11 |
| 3.1 Summary of Air Quality Observations | 11 |
| 3.2 Air Sensor Network | 14 |
| 3.3 Mean PM _{2.5} Chemical Composition for 2022 | 15 |
| 3.4 Characterisation of Ship Emissions During the Intensive Measurement Period | 17 |
| 3.5 PM _{2.5} Source Apportionment for 2022 | 25 |
| 3.6 Impact of Port Emissions on Dublin Air Quality | 26 |
| 4 Conclusions and Recommendations | 30 |
| 4.1 Conclusions | 30 |
| 4.2 Recommendations | 31 |
| References | 33 |
| Abbreviations | 36 |

List of Figures

| | | |
|--------------|---|----|
| Figure 2.1. | (a) Overview map of Dublin Port and (b) an image of the main container used throughout the campaign and the Xact container, which was used only during the intensive measurement period | 4 |
| Figure 2.2. | Map showing the locations of the nine air sensors (coloured markers) | 8 |
| Figure 2.3. | Time series of $PM_{2.5}$ measured by two collocated air sensors (AirNode, Airscape) and a reference-equivalent instrument (Fidas 200, Palas GmbH) at Station 76, “Dublin Port”, in the national monitoring network | 8 |
| Figure 2.4. | Scatter plots of $PM_{2.5}$ measured by two collocated air sensors (AirNode, Airscape) and a reference-equivalent instrument (Fidas 200, Palas GmbH) at Station 76, “Dublin Port”, in the national monitoring network | 9 |
| Figure 3.1. | Mean hourly time series for the main pollutants measured at the PortAIR measurement site during 2022 | 12 |
| Figure 3.2. | Diurnal profiles for the main pollutants measured at the PortAIR measurement site during 2022 | 13 |
| Figure 3.3. | Daily average reconstructed $PM_{2.5}$ mass concentration ($PM_{acsm+eBC}$) at the PortAIR and UCD monitoring sites for 2022 | 13 |
| Figure 3.4. | Daily $PM_{2.5}$ concentrations from the PortAIR (reconstructed in black) and Tolka Quay Road (Station 76, “Dublin Port”) sites | 14 |
| Figure 3.5. | Comparison of $PM_{2.5}$ concentrations obtained using an air sensor (AirNode 279, Airscape) with the reconstructed mass determined from the Q-ACSM+eBC data at the PortAIR site | 15 |
| Figure 3.6. | Daily $PM_{2.5}$ concentrations at the PortAIR site (reconstructed in black) | 15 |
| Figure 3.7. | A pie chart of the average species contribution (%) for 2022 is shown for (a) PortAIR and (b) UCD | 16 |
| Figure 3.8. | Time series of the high time resolution ambient measurements during the intensive PortAIR campaign | 18 |
| Figure 3.9. | The six-factor PMF solution showing the time series (a) and the diurnal profiles (b) | 19 |
| Figure 3.10. | Pie charts of the composition breakdown of PM_1 for S-Ship plumes (a) and O-Ship plumes (b), with gas data pie charts for SO_2 and NO_x also shown | 20 |
| Figure 3.11. | Pie charts showing the PMF factors and other species contributing to PM_1 (a) and source contribution estimates to PM_1 with adjusted O-Ship, S-Ship and eBC (b) | 21 |
| Figure 3.12. | Factor contribution profiles for the chosen four-factor solution from the Xact 625i PMF analysis | 21 |

| | | |
|--------------|---|----|
| Figure 3.13. | Time series for the four factors obtained from PMF analysis performed on the Xact data | 22 |
| Figure 3.14. | Diurnal profiles for the four factors obtained from PMF analysis performed on the Xact data | 22 |
| Figure 3.15. | Correlation matrix comparing the Xact PMF factors with other pollutants and the ACSM-derived PMF factors during the intensive measurement campaign | 23 |
| Figure 3.16. | Time series of data during “bat ear” ship emission events for isolated O-Ship plumes (fuel switching pattern VLSFO–MGO–VLSFO) | 24 |
| Figure 3.17. | (a) Pie chart of Q-ACSM species and eBC for 2022. (b) Bar chart of the monthly contribution of PMF resolved factors, including S-Ship, O-Ship, X-Ship, HOA, peat and OOA+ (OOA and regional sulfate), in 2022. The blue dashed highlighted area in (a) shows OA–SO ₄ ²⁻ input that is resolved by the PMF in (b). (c) Pie chart showing source contribution estimates to PM _{2.5} with adjusted O-Ship, S-Ship and eBC, as in Figure 3.11b | 25 |
| Figure 3.18. | S-Ship factor overview of (a) monthly concentrations; (b) the time series; (c) diurnal (concentration vs hour of the day) winter concentrations; (d) diurnal summer concentrations; (e) diurnal spring concentrations; and (f) diurnal autumn concentrations | 26 |
| Figure 3.19. | O-Ship factor overview of (a) monthly concentrations; (b) the time series; (c) diurnal (concentration vs hour of the day) winter concentrations; (d) diurnal summer concentrations; (e) diurnal spring concentrations; and (f) diurnal autumn concentrations | 27 |
| Figure 3.20. | Polar plots to show the relationship between wind direction/speed and PM _{2.5} concentration at four locations in the air sensor network around Dublin Port: Promenade Road (ANG5-00244), North Wall Quay (ANG5-00268), Ringsend (ANG5-00277) and PortAIR (ANG5-00279) | 28 |

List of Tables

| | | |
|------------|--|----|
| Table 2.1. | Instrumentation deployed during the PortAIR field campaign (21 December 2021 to 7 February 2023) | 5 |
| Table 3.1. | Annual mean concentrations of PM _{2.5} and pollutant gases for the calendar year 2022 at the PortAIR measurement site compared with nearby stations in the national air quality monitoring network, EU CAFE Directive limits and WHO AQG values | 11 |
| Table 3.2. | Summary statistics for PM _{2.5} measurements (corrected data) in the air sensor network during the measurement campaign | 14 |
| Table 3.3. | Summary statistics for the concentration of PM _{2.5} chemical components (expressed in $\mu\text{g m}^{-3}$) derived from online analysis using ACSM and eBC | 16 |
| Table 3.4. | Summary statistics for the concentration of PM _{2.5} chemical components (expressed in ng m^{-3}) derived from offline analysis using XRF and the OC–EC analyser | 17 |
| Table 3.5. | Mean characteristics of S-Ship and O-Ship plumes detected during the intensive measurement campaign | 20 |
| Table 3.6. | Comparison of PM _{2.5} concentrations ($\mu\text{g m}^{-3}$) measured during “Port” and “City” influenced air masses | 28 |

Executive Summary

Dublin Port is Ireland's largest freight and passenger port, handling a significant portion of the country's international trade and playing a crucial role in the national and regional economies. While ports bring significant economic and social benefits, the emissions to the atmosphere from ships, road traffic and other port-related activities contribute to climate change and air pollution, affecting the health of citizens and the environment.

Air quality is continuously measured in Dublin Port (Tolka Quay Road) and in nearby Ringsend; however, there have been no detailed studies of the sources of air pollution in the area. The principal objective of the Source Apportionment of Air Pollution in the Dublin Port Area (PortAIR) project was therefore to determine the impact of ships and other pollution sources on air quality in Dublin Port, with the aim of providing policymakers, regulatory bodies and other stakeholders with a sound scientific basis for developing targeted strategies to reduce emissions.

An extensive range of research-grade instrumentation was deployed at a monitoring location established in the north-east end of Dublin Port between December 2021 and February 2023 to provide continuous, real-time measurements of key air pollutants, including particulate matter with a diameter of less than 2.5 microns ($PM_{2.5}$), nitrogen dioxide (NO_2) and sulfur dioxide (SO_2).

The annual mean concentrations of $PM_{2.5}$, NO_2 and SO_2 at the PortAIR site in 2022 were within the current European Union Clean Air For Europe Directive limits and also within the revised annual limit values to be attained by 1 January 2030 (EU, 2008). However, the $PM_{2.5}$ and NO_2 mean concentrations did exceed the air quality guideline values set by the World Health Organization. High levels of nitrogen oxides (NO_x) were also measured at the PortAIR site, which could impact on the Bull Island Special Protection Area, situated only a few kilometres downwind.

The prevailing westerly winds generally carry emissions from ships and other port-related activities away from Dublin and over the Irish Sea. However,

data obtained from an air sensor network placed around the periphery of the port area show that in 2022 emissions from the direction of the port caused an estimated increase of up to 6% in $PM_{2.5}$ in parts of the city adjacent to the port.

Hundreds of ship plumes were monitored and characterised as discrete pollution events with known chemical markers, including SO_2 and NO_x , as well as vanadium, nickel, black carbon, organic and sulfate components in the particulates. Two main types of ship plumes were identified: one type dominated by sulfate, originating from ships using high-sulfur heavy fuel oil with an end-of-pipe scrubber system to reduce SO_2 emissions to the atmosphere; and another type dominated by organic species, emitted by ships using low-sulfur marine fuels. Ship emissions were at their highest when manoeuvring in and out of the berth, while smaller amounts of pollutants were emitted over a longer timescale when docked in port.

Source apportionment modelling was used to determine the source contributions to $PM_{2.5}$ at the PortAIR site, which showed that regional background sources (56%) were dominant, followed by ship emissions (21%), with other combustion sources such as vehicles (which includes port-related traffic) and home heating largely accounting for the remainder. Ship plumes thus constituted a significant fraction of $PM_{2.5}$ and submicron particle number concentration in the port area, were the main source of SO_2 and contributed significantly to NO_x emissions.

The increased activity linked to the planned expansion of Dublin Port is likely to lead to higher emissions from ships and road vehicles and it is therefore recommended that measures to reduce air pollution are introduced. The provision of shore-side electricity to ships at berth is one such measure that has been successfully introduced in other countries and should be given high priority. The proposed introduction of a designated Emission Control Area for the North-East Atlantic region should lead to the implementation of measures that would also result in a significant reduction in air pollution. Measures to reduce emissions from road vehicles would also be beneficial.

This research clearly demonstrated the value of sophisticated research-grade instruments and low-cost sensor networks for online continuous monitoring of particulate matter. It is therefore recommended that instruments for monitoring particle number concentration and size distribution are used regularly to provide a detailed assessment of the presence and sources of ultrafine particles, which are especially harmful to health. Further efforts should also be made

to deploy PM_{2.5} sensor networks to assess the spatial variation of air pollution in urban locations, including in areas such as ports, where there are many local sources. Finally, it is recommended that future field measurement campaigns utilise online elemental analysis to provide a more complete understanding of both the anthropogenic and natural sources of particulate matter.

1 Introduction

1.1 Background

Ports are essential infrastructures for international trade and are critical to economies around the world. Indeed, marine transport (shipping) accounts for around 80% of external trade both in the European Union (EU) and globally, underlining its strategic value. Ports play an equally important role nationally by supporting the exchange of goods within the Irish market, serving as hubs of economic activity and providing employment. They are also vital gateways for the movement of people by passenger ferries and cruise ships, supporting the travel and tourism industry. While the maritime sector brings significant economic and social benefits, it also has a negative impact on the environment and contributes to climate change and air pollution, affecting the health of citizens.

Ships emit significant amounts of sulfur¹ dioxide (SO₂), nitrogen oxides (NO_x), primary particulate matter (PM), carbon dioxide (CO₂) and a range of volatile organic compounds. Maritime transport contributed 11% of the total EU greenhouse gas emissions from transport in 2022. Air pollutant emissions from the sector are significant and represented 39% of NO_x, 88% of SO₂ and 43% of PM_{2.5} (particulate matter with a diameter less than 2.5 microns) as proportions of EU transport emissions in 2022 (EEA, 2025a, 2025b). Chemical reactions in the atmosphere between NO_x and SO₂, and ammonia gas primarily emitted from agricultural activities, also lead to the formation of secondary inorganic PM. The primary and secondary pollutants derived from shipping emissions contribute to adverse human health effects, influence climate and cause further environmental damage through acidification and eutrophication. For example, shipping emissions in the Atlantic Ocean are estimated to account for 19% of sulfur and 16% of nitrogen deposition in Ireland (EEA, 2013). Moreover, global health impact assessments have estimated the number of annual deaths due to shipping and

port-sourced air pollution to be in the range of 45,000–265,000 (Mueller *et al.*, 2023).

Regulations to control the emissions from ships have been introduced to reduce the impact of marine transport on human health and on the environment. The International Maritime Organization regulates air pollution from shipping through Annex VI to the Marine Pollution Convention (MARPOL Training Institute, 2006). Annex VI includes measures to reduce NO_x and PM emissions, as well as regulations on the sulfur content of fuel. Since 1 January 2020, the global upper limit for sulfur in fuels is 0.5% (mass by mass (m/m)). In addition, there are several designated Sulfur Emission Control Areas where the upper limit for sulfur is 0.1%: (i) the Baltic Sea Area, (ii) the North Sea Area, (iii) the North American Sea Area and (iv) the US Caribbean Sea Area. Under the EU Sulphur Directive, ships at berth in EU ports must use marine fuels with a sulfur content not exceeding 0.1% and complete any necessary fuel changeover operation as soon as possible after arrival at berth and as late as possible before departure.

Compliance with these regulations is typically achieved by using low-sulfur fuels, which are classified into two categories: very-low-sulfur fuel oil (VLSFO), with a sulfur content of <0.5%, and ultra-low-sulfur fuel oil (ULSFO), with a sulfur content of <0.1%. However, ships are also considered compliant if they use heavy fuel oil (HFO), with a sulfur content up to 3.5%, in combination with exhaust gas cleaning systems (scrubbers) fitted to “scrub” the SO₂ from their emissions. A common wet scrubber design uses alkaline solution, often seawater pumped from below the ship, to spray through the exhaust system to scavenge and reduce SO₂ emissions. In open-loop scrubber systems, the wastewater is discharged directly overboard where it may cause pollution, whereas in closed-loop scrubber systems the water is recirculated and the wastewater is disposed of according to regulations.

¹ In the late 20th century, the International Union of Pure and Applied Chemistry declared that the single spelling of sulfur is preferred. Following best practice in scientific publishing, sulfur is used throughout this report, except where sulphur is in the title of a document or publication, such as the EU Sulphur Directive.

1.2 Air Pollution in Port Areas

In port areas, ship emissions are produced when the vessels are arriving and departing, manoeuvring in and out of berths, and hoteling – a term used to describe the time that ships spend at berth for unloading/loading of cargo and passengers. At berth, ships switch off the main engines but use auxiliary engines and boilers for power. Other non-ship sources of air pollution in ports include heavy-duty goods vehicles, passenger road traffic and the use of port machinery, such as cranes. Industries located in the area, which include gas and oil refineries, chemical plants, power stations and incinerators, can also contribute to local emissions.

The wide variety of air pollution sources in port areas makes identification and quantification of the individual sources challenging. This is particularly true for combustion particles from ships and road vehicles, which have similar chemical components, such as organic compounds and black carbon, and may also be intrinsically related, for example primary ship emissions and secondary formation of aerosol from ship-related precursor gases. However, a combination of chemical analysis methods and source apportionment modelling can be used to successfully estimate the contribution of specific sources to the ambient PM measured in port areas. For example, 3.7–6.1% of organic aerosol (OA) was related to shipping and industrial plumes in Marseille, France (Chazeau *et al.*, 2022); 1.5% of $PM_{2.5}$ and 18% of particle number concentration were related to shipping traffic in Cork Harbour, Ireland (Healy *et al.*, 2010; O'Connor *et al.*, 2013); shipping emissions were 5–14% of $PM_{2.5}$ on the Spanish coast (Pandolfi *et al.*, 2011; Viana *et al.*, 2009); and shipping emissions were 4–13% of primary $PM_{2.5}$ in Shanghai Port and Hong Kong SAR Port (Yau *et al.*, 2013; Zhao *et al.*, 2013) and 25% overall in Hong Kong SAR Port (Yau *et al.*, 2013). In Ningbo-Zhoushan Port, China, 18% of polycyclic aromatic hydrocarbons in $PM_{2.5}$ were found to come from HFO combustion (Hong *et al.*, 2023), and shipping emissions contributed 6–22% of volatile organic compounds in the Pearl River Delta region (Tong *et al.*, 2024).

Traditional methods for chemical analysis of PM include the determination of organic compounds, water soluble ions and elements using offline methods such as gas/liquid chromatography mass spectrometry, ion chromatography and X-ray fluorescence (XRF),

respectively. However, the aerosol particles need to be collected onto filters, typically over a 24-hour period, and this relatively poor time resolution is often not sufficient to identify short-lived emissions like ship plumes. High time resolution measurements of aerosol chemical composition using online instruments such as the aerosol chemical speciation monitor (ACSM) and Xact Ambient Continuous Multi-Metals Monitor (Xact) are therefore better suited to identifying different emission sources in port areas. Different analysis techniques can be used to perform source apportionment; one leading type of multivariate analysis for high-resolution aerosol composition is positive matrix factorisation (PMF), which can resolve distinct primary as well as secondary aerosol sources (e.g. Chazeau *et al.*, 2022; Yau *et al.*, 2013).

A key aspect of air pollution studies in port areas is the ability to identify shipping emissions. Many previous studies have used vanadium (V) and nickel (Ni) as chemical tracers to identify primary emissions from combustion of HFO (Agrawal *et al.*, 2009; Healy *et al.*, 2009; Mueller *et al.*, 2011; Zhao *et al.*, 2013), and concentration ratios ranging from 2.5 to 4.0 are associated with typical ship emissions (Mazzei *et al.*, 2008; Pandolfi *et al.*, 2011; Viana *et al.*, 2009). Other markers for ship emissions include black carbon, sulfate (SO_4^{2-}) and OA. However, the switch from HFO to fuels with a lower sulfur content and the increased use of scrubbers, prompted by the International Maritime Organization regulations, will cause the chemical composition of ship emissions to change.

The use of scrubbers to reduce SO_2 emissions from ships using HFO is expected to produce particles with similar chemical signatures to those in untreated HFO exhaust emissions, but with increased amounts of SO_4^{2-} (Yang *et al.*, 2021). The use of ULSFO instead of HFO has been shown to reduce the mass concentration of PM by 67% and SO_2 emissions by 80%, and result in an overall decrease in volatile organic compounds, including the heavier and carcinogenic polycyclic aromatic hydrocarbons (Zetterdahl *et al.*, 2016). However, this transition has also been shown to increase the production of monoaromatic and lighter polyaromatic hydrocarbon compounds (Zetterdahl *et al.*, 2016). Despite reductions in many pollutants, the lowering of the sulfur fuel content is unlikely to lead to significant changes in either the total particle number concentration or the black carbon mass concentration

(Zetterdahl *et al.*, 2016). Studies have shown that low-sulfur fuels contain much lower amounts of metals from the refinery process and therefore will not have the typical chemical markers of HFO traditionally used for tracing ship emissions (Anders *et al.*, 2023; Czech *et al.*, 2017). While it has been proposed that lubricant oil from marine engines could provide a fuel-independent pool of possible marker substances (Eichler *et al.*, 2017), new studies are urgently needed in port areas to derive alternative markers or chemical profiles for ship emissions, as well as diagnostic ratios for both particle-bound and volatile organics (Czech *et al.*, 2017).

1.3 The PortAIR Project

Dublin Port is the largest port in Ireland, classified as a Tier 1 medium port. In 2019, it handled 49.5% ($\sim 26.3 \times 10^6$ gross tonnage of goods) of Irish freight (CSO, 2019). For context, the largest port in the EU, Rotterdam Port, has 18 times this capacity. Dublin Port expects to double its capacity by 2040, at a 3.3% expansion rate per annum (Dublin Port Masterplan 2040; DPC, 2018). Dublin Port is adjacent to the urban centre of Dublin city (<5 km), where source apportionment of the ambient PM has been studied at both urban background and roadside monitoring locations (Lin *et al.*, 2018, 2019; Ovadnevaite *et al.*, 2021). Dublin Port is directly downwind of the

prevailing westerlies (south-westerlies) and for this reason is impacted by air pollution from both the port and the city centre of Dublin. Air pollution in the port area is measured at two sites in the national ambient air quality monitoring network: “Dublin Port” or Station 76, which is located on Tolka Quay Road on the north side of the River Liffey, and “Ringsend” or Station 17, which is located in Ringsend on the south side of the Liffey (EPA, 2025). Dublin Port Company has also conducted several air quality assessments over the years; however, there have been no detailed studies of the sources of air pollution in the Dublin Port area.

The overall aim of the PortAIR project is to determine the impact of ship emissions on air quality in the Dublin Port area. This will be achieved through a combined measurement–analysis approach, involving (i) continuous year-long monitoring of the chemical composition of PM in real time; (ii) a multi-instrument intensive field campaign conducted during the height of shipping activity; and (iii) detailed source apportionment models providing robust quantitative estimates of the impact of shipping emissions and other sources affecting air quality in the area. The results will provide Dublin Port Company and other stakeholders (Dublin City Council, the Environmental Protection Agency, government departments) with a sound scientific basis for developing strategies and policies to reduce air pollution from port-based activities.

2 Methods

2.1 Field Measurements

Field measurements of atmospheric particles and gaseous pollutants were conducted at a monitoring site (53.348439N, 6.194657W) established in the north-east end of Dublin Port. The location was downwind of most port activity and close to the ferries, which are a

major daily source of shipping emissions. The location of the monitoring site in relation to the ferry terminals and other areas of the port is shown in Figure 2.1. The field site was in operation from 21 December 2021 to 7 February 2023, with an intensive measurement period taking place from 16 December 2022 to the end of the monitoring campaign.



Figure 2.1. (a) Overview map of Dublin Port (satellite image credit: Imagery ©2024 Airbus, Landsat/Copernicus, Maxar Technologies, Map data ©2024 Google); and (b) an image of the main container used throughout the campaign and the Xact container, which was used only during the intensive measurement period (image credit: Kirsten Fossum).

2.2 Instrumentation

A wide range of instrumentation for measuring atmospheric particles, gases and other air quality parameters was deployed during the 14-month field measurement campaign (Table 2.1). The instruments were housed in two customised containers, both fitted with appropriate sampling inlets (Figure 2.1). All instruments were operated on a continuous basis, with the measured parameters typically analysed to yield hourly values. Occasional periods of downtime were required for calibration and repair of the instruments. Further details concerning the operation and analysis of data generated by the key instruments are provided in the following sections.

2.2.1 Q-ACSM

The quadrupole aerosol chemical speciation monitor (Q-ACSM; Aerodyne Research Inc.) measured the mass concentrations of non-refractory species, including OA, SO_4^{2-} , nitrate (NO_3^-), ammonium (NH_4^+) and chloride (Cl^-) in near real time (Ng *et al.*, 2011). $\text{PM}_{2.5}$ composition was measured for most of the field campaign (21 December 2021 to 13 December 2022), but, due to technical issues, a switch to PM

with a diameter of less than 1 micron (PM_{10}) was made at the start of the intensive measurement period (16 December 2022 to 27 January 2023). The Q-ACSM instruments had a standard vaporiser and were calibrated and maintained in accordance with the standard protocol developed by the COST Action CA16109 (Chemical On-line Composition and Source Apportionment of Fine Aerosol (COLOSSAL)). In this study, the Q-ACSM was operated using a carrier flow rate of $2.5 (\pm 0.2)$ litres per minute (LPM) with a distance from inlet to Q-ACSM of approximately 2 metres, to keep particle losses to a minimum. A monotube Nafion membrane dryer was installed to maintain relative humidity of the sample air in the range 20–40%. The instrument was operated at a time resolution of just over 5 minutes (five sets of one sample and one filter measurement scan). Further details of the instrument operation and calibration procedures are reported in the literature (ACTRIS, 2021; Fossum *et al.*, 2024).

2.2.2 Aethalometer AE33

The aethalometer (model AE33, Aerosol Magee Scientific) collects particles on filter tape and measures the attenuation of light at seven different wavelengths

Table 2.1. Instrumentation deployed during the PortAIR field campaign (21 December 2021 to 7 February 2023)

| Instrument (manufacturer and model) | Parameter(s) measured | Temporal resolution |
|---|---|---------------------------|
| Q-ACSM (Aerodyne Research Inc.) | Chemical composition of $\text{PM}_{2.5}$ ^a or PM_{10} ^b | 5 min |
| SMPS (TSI Inc., model 3081) | Particle number concentration (10–480 nm) | 3 min |
| Optical particle sizer (TSI Inc., model 3330) | Particle number concentration (300–10,000 nm) | 3 min |
| Seven-wavelength aethalometer (Aerosol Magee Scientific, model AE33) | Black carbon concentration | 1 min |
| Xact 625 Ambient Continuous Multi-Metals Monitor (Cooper Environmental) | Metals and other elements in $\text{PM}_{2.5}$ ^b | 1 h |
| High-volume sampler (Digitel, model DHA 80) | Collection of $\text{PM}_{2.5}$ | 24 h and 6 h ^c |
| NO_x analyser (Teledyne Technologies, model T200A) | NO and NO_x mixing ratio | 5 min |
| SO_2 analyser (Teledyne Technologies, model T100) | SO_2 mixing ratio | 1 min |
| CO analyser (Teledyne Technologies, model T300) | CO mixing ratio | 5 min |
| O_3 analyser (Thermo Fisher Scientific, model 49i) | O_3 mixing ratio | 5 min |
| Air sensors (Airscape, AirNode) | $\text{PM}_{2.5}$, NO_2 , O_3 , CO_2 , temperature, relative humidity | 1 min |
| Weather station (Casella, Nomad) | Wind speed and direction, pressure, relative humidity, temperature | 5 min |

^a21 December 2021 to 13 December 2022.

^b16 December 2022 to 27 January 2023.

^c20 January 2023 to 7 February 2023.

CO, carbon monoxide; **NO**, nitric oxide; **NO₂**, nitrogen dioxide; **O₃**, ozone; **SMPS**, scanning mobility particle sizer.

(370, 470, 520, 590, 660, 880 and 950 nm) to provide optical absorption coefficients at 1-minute time resolution. The AE33 uses a dual spot measurement technique that allows for the correction of filter loading effects by aerosol in real time (Drinovec *et al.*, 2015). The change in optical attenuation at 880 nm is used to determine the concentration of light-absorbing equivalent black carbon (eBC) (Bond *et al.*, 2013; Petzold *et al.*, 2013) using the standard mass-specific absorption cross section of $7.77 \text{ m}^2 \text{ g}^{-1}$ and an optical enhancement factor (*C*) of 1.57 for the tetrafluoroethylene-coated glass fibre tape (Drinovec *et al.*, 2015). In this study, the aethalometer was operated using a flow rate of $5 (\pm 0.4) \text{ LPM}$. The rolling 15-minute average was calculated from the 1-minute data to reduce noise. This rolling average was used to interpolate eBC concentrations that matched Q-ACSM data points in time.

2.2.3 Xact

The Xact 625 Ambient Continuous Multi-Metals Monitor (Cooper Environmental) was used in the intensive measurement period to determine the concentration of selected elements (arsenic (As), barium (Ba), calcium (Ca), cadmium (Cd), cerium (Ce), Cl, chromium (Cr), copper (Cu), iron (Fe), potassium (K), manganese (Mn), molybdenum (Mo), Ni, lead (Pb), platinum (Pt), sulfur, antimony (Sb), selenium (Se), silicon (Si), strontium (Sr), titanium (Ti), V and zinc (Zn)) in $\text{PM}_{2.5}$ at 1-hour time resolution. The $\text{PM}_{2.5}$ samples were collected onto Teflon tape and subsequently analysed with energy dispersive XRF using a rhodium anode (50 kV, 50 W) X-ray source and Si drift detector (Furger *et al.* 2017; Tremper *et al.*, 2018). Daily automated quality assurance procedures were performed at midnight. Further quality assurance measures, such as flow checks and external calibrations, were performed at the start and end of the intensive measurement period. The instrument was operated at a flow rate of 16.67 LPM and the inlet tube heated to 45°C .

2.2.4 Scanning mobility particle sizer

A scanning mobility particle sizer (SMPS) (TSI Inc.) was used to measure the number–size distribution of ambient aerosol particles. Particles passing through the system are charge neutralised (electrical ionizer model 1090, MSP Corp), then sized by electrical

mobility through a differential mobility analyser (model 3080, TSI Inc.) and finally counted by a condensation particle counter (model 3010, TSI Inc.). The SMPS was operated by passing sample air through a multi-tube Nafion membrane and into the differential mobility analyser at a sample flow of $\sim 1 \text{ LPM}$ and a sheath flow of 5 LPM (Collins *et al.*, 2004). The scan duration was set to 3–5 minutes using the TSI Inc. AIM software (release version 9.0.0.0), and charge correction was applied. Data were generally analysed to yield average hourly and daily values.

2.2.5 Gas analysers

Gases were measured throughout the field campaign using automated gas analysers. The Teledyne Technologies model 200A analyser measured mixing ratios of nitric oxide (NO) and NO_x , and by calculation nitrogen dioxide (NO_2), in parts per billion (ppb) at a time resolution of 5 minutes. The Teledyne Technologies model T100 analyser measured SO_2 mixing ratios (ppb) at 1-minute time resolution. Due to a drift in the SO_2 baseline over the 14-month campaign, local minima were used to develop a polynomial baseline correction that was subsequently applied to the SO_2 data. Initially, a simple linear correction was considered; however, due to the stepped nature of the drift, this was not deemed to be an adequate correction. The Teledyne Technologies model T300 analyser measured the mixing ratio of carbon monoxide (CO) in parts per million (ppm) at 5-minute time resolution. The Thermo Fisher Scientific model 49i analyser measured ozone (O_3) (ppb) at 5-minute time resolution. Conversion of gas mixing ratios to concentrations was performed using the following expressions derived using a temperature of 20°C and pressure of 1 atm: $1 \text{ ppb} = 1.9125 \mu\text{g m}^{-3}$ for NO_2 ; $1 \text{ ppb} = 1.28 \mu\text{g m}^{-3}$ for NO; $1 \text{ ppm} = 1.15 \text{ mg m}^{-3}$ for CO; and $1 \text{ ppb} = 1.96 \mu\text{g m}^{-3}$ for O_3 .

2.2.6 Filter sampling and offline analysis

The high-volume sampler (model DHA 80, Digital) was used to collect samples of $\text{PM}_{2.5}$ onto quartz fibre filters (Pallflex, 150 mm diameter), which had been pre-baked for 3 hours at 850°C . A flow rate of 500 LPM and a sampling frequency of 24 hours (00:00 to 23:59) was used, except for the period 20 January 2023 to 7 February 2023, where a 6-hour sampling frequency was used. Following collection, the filters were

individually packed and stored in a freezer at -18°C . A total of 466 quartz filters were collected over the period 22 December 2021 to 7 February 2023. Circular portions (47 mm diameter) of each filter, including blanks, were sent to the Environmental Radioactivity & Aerosol Technology for Atmospheric & Climate Impact (ENRACT) laboratory in the Institute of Nuclear & Radiological Sciences and Technology, Energy & Safety in Athens, Greece, for offline analysis. Two analytical methods were employed: XRF spectrometry for elemental analysis of major and trace metals, and the thermo-optical method for assessing organic carbon (OC) and elemental carbon (EC).

A high-resolution energy dispersive XRF 3D optics spectrometer (Epsilon 5, Malvern Panalytical) was used for the analysis of $\text{PM}_{2.5}$ quartz fibre filters. The spectrometer consists of a side-window X-ray tube with a W/Sc anode and a beam spot size of 21 mm. The characteristic X-ray radiation emitted by the sample is analysed by a germanium (Ge) detector with a measured energy resolution of approximately 150 eV full width at half maximum at the Mn-K α peak (i.e. 5.89 keV). The spectrometer provides a selection of six secondary targets (calcium fluoride (CaF_2), Ge, potassium bromide (KBr), Mo, lanthanum hexaboride (LaB_6) and aluminum oxide (Al_2O_3)) that can polarise the primary tube radiation, thus minimising the spectral background (in triaxial geometry, the doubly scattered tube radiation is minimised at the detector direction). All measurements were conducted under vacuum and the total acquisition time was approximately 50 minutes per sample. Fourteen elements were determined by the XRF method, namely sodium (Na), S, Cl, K, Ca, Ti, V, Fe, Ni, Cu, Zn, bromine (Br), Ba and Pb.

Thermo-optical transmittance analysis was performed using the Lab OC-EC Aerosol Analyser (Sunset Laboratory Inc.) and the EUSAAR2 (European Supersites for Atmospheric Aerosol Research) protocol, following the quality assurance/quality control procedures described in EN 16909: 2017. Quartz filter samples were heated to 650°C in helium (He), at first, and then to 850°C in a mixture of 2% oxygen (O_2) in He, using the controlled heating ramps of the EUSAAR2 thermal protocol. OC evolved in the inert atmosphere, while EC was oxidised in the He- O_2 atmosphere. Charring correction was applied by monitoring the sample transmittance throughout the heating process. The limit of detection was

$0.02\text{ }\mu\text{g m}^{-3}$ of carbon. Field blanks were also analysed and were found to be within the acceptable values set in EN 16909: 2017. The expanded uncertainty was calculated equal to 15% for OC and 23% for EC.

2.2.7 Air sensor network

Nine air sensors (AirNode, Airscape) were deployed at various locations across the port to measure the spatial and temporal variability of air pollution, with a focus on $\text{PM}_{2.5}$. The selected locations are shown in Figure 2.2 and include the PortAIR monitoring site and the two closest air quality monitoring stations in the national network, situated in Ringsend (Station 17) and Dublin Port (Station 76). The other locations were Irish Ferries Terminal 1; Promenade Road; Dublin Port Company headquarters; North Wall Quay; and Poolbeg Yacht and Boat Club. The sensors were deployed in the network from 16 April 2022 to 7 February 2023.

Prior to deployment throughout the port, the sensors were collocated at the PortAIR site for around 1 month to check that the inter-sensor variability was sufficiently low. Evaluation of sensor performance was carried out after the field measurement campaign by deploying the two sensors situated at the PortAIR monitoring location alongside the PM reference instrument (Fidas 200, Palas GmbH) at the nearby monitoring station in Dublin Port (Station 76). The time series and correlation plots for data collected over the period March to June 2023 are shown in Figures 2.3 and 2.4, respectively.

From this comparison there is excellent correlation between both sensors and the reference-equivalent instrument; however, the sensors underestimated $\text{PM}_{2.5}$ concentrations by 20%. Given the excellent inter-sensor comparison observed both at the beginning and end of the measurement campaign, it was decided to apply a correction factor of 20% to the data recorded by each of the sensors in the network.

2.2.8 Meteorology station

Wind direction, wind speed, air temperature, air pressure, relative humidity, rainfall and solar radiation measurements were made using a weather station (Casella, model Nomad) mounted to the top of the main container. The measured wind speed and direction compared well with the data available from

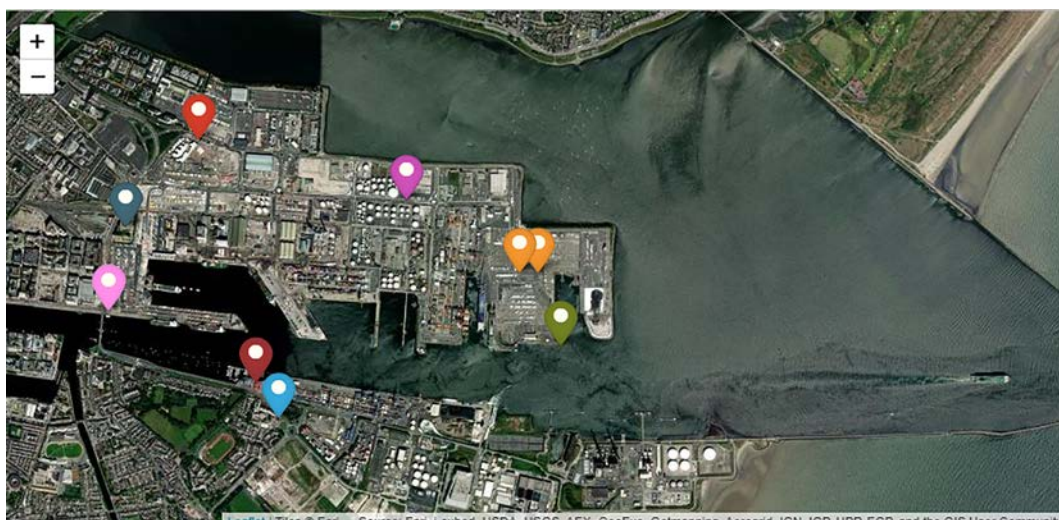


Figure 2.2. Map showing the locations of the nine air sensors (coloured markers). Two of the sensors were located at the PortAIR monitoring site (orange markers), and a sensor was located at the air quality monitoring stations in Ringsend and Dublin Port (blue and purple markers, respectively).

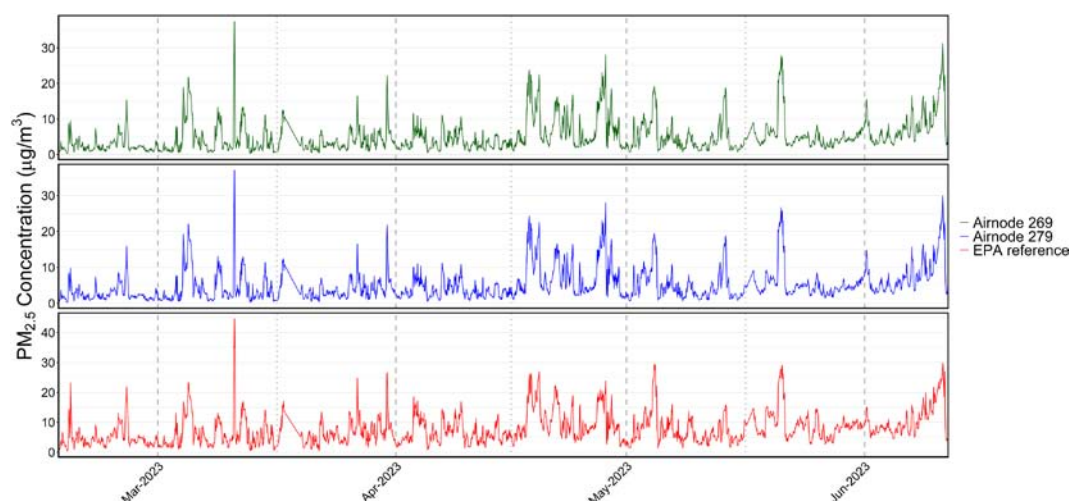


Figure 2.3. Time series of $PM_{2.5}$ measured by two collocated air sensors (AirNode, Airscape) and a reference-equivalent instrument (Fidas 200, Palas GmbH) at Station 76, “Dublin Port”, in the national monitoring network.

the nearest Met Éireann meteorological station located at Dublin Airport, less than 10 km north of Dublin Port.

2.3 Source Apportionment

2.3.1 Q-ACSM

PMF (Paatero, 1997) was used to apportion the OA measured by the Q-ACSM into different emission source categories. The PMF was conducted on the original 5-minute time resolution data using the Multilinear Engine version 2 (ME-2) (Paatero, 1999)

implemented in the software SoFi (version 9.4.10) (Canonaco *et al.*, 2013). Unconstrained PMF solutions were first considered and analysed for any physically meaningful separation of factors. Using the information from the unconstrained PMF and prior knowledge of the Dublin area, reference mass spectral profiles were used to constrain the ME-2 algorithm (Canonaco *et al.*, 2013) and these reference profiles were left to vary within specified limits using either the limits approach (Lin *et al.*, 2021) or the a -value approach. Different from the a -value approach, where all m/z in the mass spectrum vary uniformly, in the limits approach, each

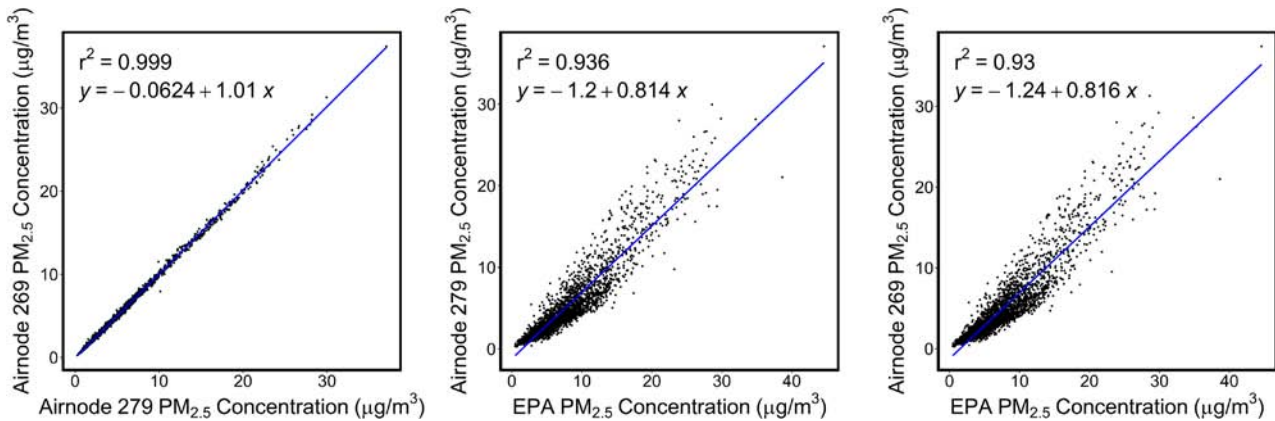


Figure 2.4. Scatter plots of $PM_{2.5}$ measured by two collocated air sensors (AirNode, Airscape) and a reference-equivalent instrument (Fidas 200, Palas GmbH) at Station 76, “Dublin Port”, in the national monitoring network. Inter-sensor comparison is excellent; however, both sensors under-report $PM_{2.5}$ by approximately 20%.

m/z in the input mass spectrum was individually varied. For example, one m/z may have a variation of 2% while another may vary by 40%. This approach is commonly used to capture variation in emission conditions, such as different stove type for burning solid fuels, and can be found when combining multiple profiles into a mean mass spectrum with standard deviations at each ion. The limits were then set for each m/z , with the lower limit and upper limit at plus or minus a standard deviation. To assess the robustness of the PMF solution, a bootstrap resampling strategy (Davison and Hinkley, 1997; Efron, 1979; Paatero *et al.*, 2014; Ulbrich *et al.*, 2009) was employed on the data obtained during the intensive measurement period. This method evaluated the statistical uncertainty of the solution, which could, for example, arise from variations in emission sources.

For the PM_1 PMF analysis, organic and SO_4^{2-} ions were combined in a matrix. Details of how the combined OA- SO_4^{2-} matrix was constructed and how SO_4^{2-} was added back to factors after running PMF can be found in Fossum *et al.* (2024). For the $PM_{2.5}$ Q-ACSM data collected throughout the whole campaign, a seasonal PMF was run using constrained profiles obtained from analysis of the data-intensive measurement campaign. Additionally, the SO_4^{2-} fragmentation pattern differed from that observed using the PM_1 Q-ACSM, while remaining robust across different acidity and ambient conditions. Therefore, the remaining ion fragments for SO_4^{2-} were calculated based on the ion ratio m/z 64 for the $PM_{2.5}$ Q-ACSM (instead of the m/z 80 ratio, as was done for PM_1),

as this m/z value had the lowest variance and a high signal-to-noise ratio.

2.3.2 Xact

PMF was performed on the Xact 625i metal concentration data using SoFi version 6.B packaged in Igor Pro v6.37 (WaveMetrics Inc.). PMF was run to resolve 1 to 10 factors, with no *a priori* information provided. Initial analysis highlighted that four-factor solutions reconstructed approximately 92% of the Xact data, while the addition of further factors produced inconsistent solutions that either split the factors resolved in the four-factor solution or separated single elements due to one or two extreme events. However, the solutions with additional factors were not very stable, revealing ambiguity in the mathematical separation. The stability of the four-factor solutions was shown to be robust when investigated by bootstrap analysis. The bootstrap analysis showed extremely low variance, with standard deviations of elements in four factors ranging from 1.2×10^{-3} to $1.7 \times 10^{-7} \text{ ng/m}^3$. Additionally, the four-factor solution was most realistic when compared with external tracers and the results of the Q-ACSM PMF. For these reasons, a four-factor solution is presented in this report.

2.4 Reconstruction of $PM_{2.5}$ Mass Concentration

The reconstructed $PM_{2.5}$ mass concentration was determined by adding together the mass

concentrations of the individual chemical components continuously measured by the ACSM (OA, NO_3^- , SO_4^{2-} , NH_4^+ and Cl^-) and AE33 (eBC). Reconstructed $\text{PM}_{2.5}$ was calculated at a time resolution of about 5 minutes to match the ACSM measurements. The 1-minute resolution used by the AE33 can lead to noisy data, and a 15-minute rolling average of the eBC

mass concentration was therefore applied to maintain the high resolution of short-lived pollution peaks, while reducing noise during periods where background concentrations were low. The rolling average eBC was interpolated to the timestamp of the ACSM measurements.

3 Results and Discussion

3.1 Summary of Air Quality Observations

The mean concentration of pollutant gases and PM_{2.5} at the PortAIR measurement site for the calendar year 2022 are given in Table 3.1, along with equivalent data obtained at the nearby national air quality network stations, Dublin Port (Station 76) and Ringsend (Station 17). The results show that annual PM_{2.5} concentrations observed at all three sites were within the current EU Clean Air For Europe (CAFE) Directive limits, as well as the reduced annual mean limit value of 10 µg m⁻³ to be attained by 1 January 2030 (EU, 2008). The annual mean concentrations of both NO₂ and SO₂ were also within their current annual CAFE Directive limits, although the NO₂ concentration measured at Dublin Port (Station 76) exceeded the reduced annual mean limit value of 20 µg m⁻³ to be attained by 1 January 2030. As for many urban locations in Ireland, the annual mean concentrations of PM_{2.5} and NO₂ exceeded the World Health Organization (WHO) air quality guideline (AQG) values at all three sites.

High levels of NO_x (NO + NO₂) were also measured at the three sites; however, the annual critical load value of 30 µg m⁻³ for NO_x (NO + NO₂) is for protection of ecosystems and is not directly applicable to these urban monitoring locations. Nevertheless, it is included here because there are some Special Areas

of Conservation close to Dublin Port. Neither CO nor O₃ have legislated annual limit values, but they do have limits on shorter timescales.

The hourly time series for each of the main pollutants measured at the PortAIR site are shown in Figure 3.1. Of particular interest is the sustained pollution event that lasted from 21 March 2022 to 30 March 2022, when Ireland experienced a period of stable atmospheric conditions, with light winds from the south-east direction. This pollution event was characterised by elevated PM_{2.5} concentration but no significant increase in any of the gases. The Q-ACSM data show that the chemical composition of the PM_{2.5} was dominated by secondary OA, and, given the prevailing weather conditions, this pollution event is attributed to the long-range transport of material from outside Ireland and the UK. The short-lived spikes where PM_{2.5} concentration reached at least 40 µg m⁻³, such as those in January and November, occurred in the night-time, between 19:00 and 01:00, and are attributed to emissions from local solid fuel burning.

High concentrations of NO were observed at the PortAIR site throughout the year, with numerous peaks above 100 µg m⁻³ and some up to 300 µg m⁻³. Fresh exhaust emissions from road and ferry traffic are major sources of NO pollution, while significant spikes in NO often coincided with elevated SO₂ concentrations, notably in March, October and

Table 3.1. Annual mean concentrations of PM_{2.5} and pollutant gases for the calendar year 2022 at the PortAIR measurement site compared with nearby stations in the national air quality monitoring network, EU CAFE Directive limits and WHO AQG values

| Pollutant | PortAIR site | Station 17 (Ringsend) | Station 76 (Dublin Port) | EU CAFE Directive limit | WHO AQG |
|---|--------------|-----------------------|--------------------------|------------------------------|---------|
| PM _{2.5} (µg m ⁻³) | 7.6 | 7.7 | 8.3 | 20 (annual mean) | 5 |
| NO ₂ (µg m ⁻³) | 13.6 | 19.1 | 27.3 | 40 (annual mean) | 10 |
| NO _x (µg m ⁻³)* | 32.8 | 34.1 | 57.5 | 30 (annual mean)* | — |
| O ₃ (µg m ⁻³) | 40.7 | — | — | 120 (maximum daily 8 h mean) | — |
| SO ₂ (µg m ⁻³) | 1.27 | 2.9 | 1.7 | 20 (annual mean) | — |
| CO (mg m ⁻³) | 0.218 | — | — | 10 (8 h mean) | — |

Note that the O₃ CAFE Directive value is a target not a limit, and NO_x is a critical load value not a limit.

*Not applicable to Dublin Port, as NO_x limits are for protection of ecosystems. Sampling site should be more than 5 km away from built-up areas. However, it is included here as Dublin Port is directly encompassed by SPA: 004024 – South Dublin Bay and River Tolka Estuary Special Protection Area (EU Birds Directive (2009/147/EC)), as well as surrounded by several Special Areas of Conservation (SAC: 000206, 000210 and 003000; EU Habitats Directive).

—, no data.

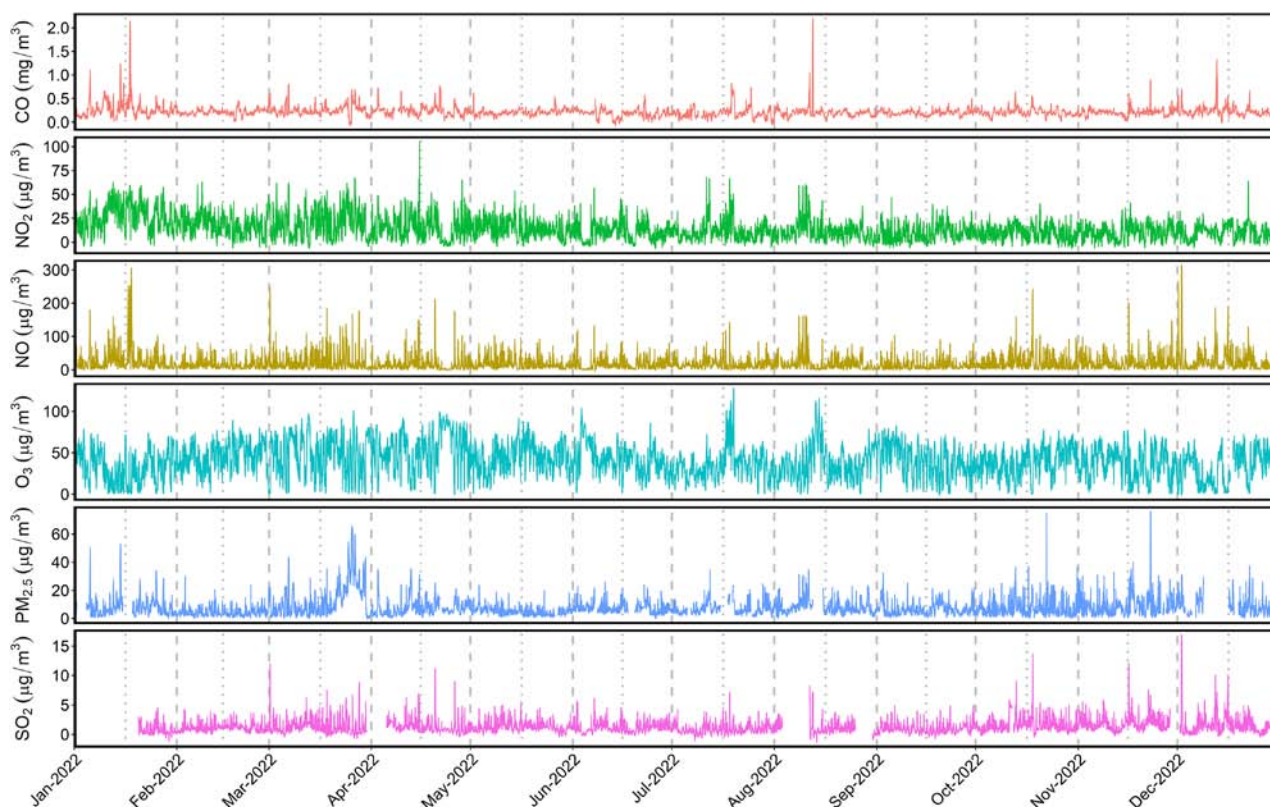


Figure 3.1. Mean hourly time series for the main pollutants measured at the PortAIR measurement site during 2022.

December, highlighting the influence of ship emissions at the measurement site.

The diurnal profiles for the pollutants provide further insight into the trends and likely sources of each species (Figure 3.2). NO and NO₂ concentrations are clearly influenced by vehicle emissions, with morning and evening peaks corresponding to typical traffic patterns. Interestingly, the evening peak for NO is smaller than the morning peak, and the whole profile is more like that for SO₂, which has a large morning peak and less intense peaks occurring around midday and in the evening, correlating well with emissions from ships and ferry traffic. PM_{2.5} also has peaks in the morning and during the middle of the day; however, the highest levels are observed in the evening, highlighting the impact of solid fuel combustion on particulate concentrations. As expected, O₃ is highly anti-correlated with NO and NO₂ due to the well-known chemical reactions between these species.

The PM_{2.5} mass concentration reported in Table 3.1 is the reconstructed mass calculated from the sum of the Q-ACSM species and eBC concentrations (section 2.4). This is a well-established approach for determining PM_{2.5} mass and is confirmed by

good agreement for volume comparisons made between the reconstructed PM_{2.5} and SMPS hourly measurements (slope 1.2, orthogonal fitting, $r^2=0.6$). The reconstructed PM_{2.5} for the PortAIR site is shown with the equivalent data obtained at the monitoring site at University College Dublin (UCD), located around 5 km from Dublin Port (Figure 3.3). The UCD site is an urban background location just south of Dublin city centre (53.3089 N, -6.2242 W), close to main roads and residential areas (Lin *et al.*, 2018, 2020). Overall, the daily PM_{2.5} values at the PortAIR and UCD sites compare very well (slope of 0.9 and $r^2=0.74$), but the PortAIR annual PM_{2.5} concentration (7.6 µg m⁻³) is higher than that at UCD (4.9 µg m⁻³). The number of days when PM_{2.5} was above the WHO recommended 24-hour AQG value of 15 µg m⁻³ was 25 for the PortAIR site and 21 for the UCD site.

The daily reconstructed PM_{2.5} concentrations are also compared with the values measured using the reference monitor (Fidas 200, Palas GmbH) located at the designated Dublin Port monitoring site (Station 76) on Tolka Quay Road (Figure 3.4). There is reasonably good agreement between the two sites, especially considering the difference in both location

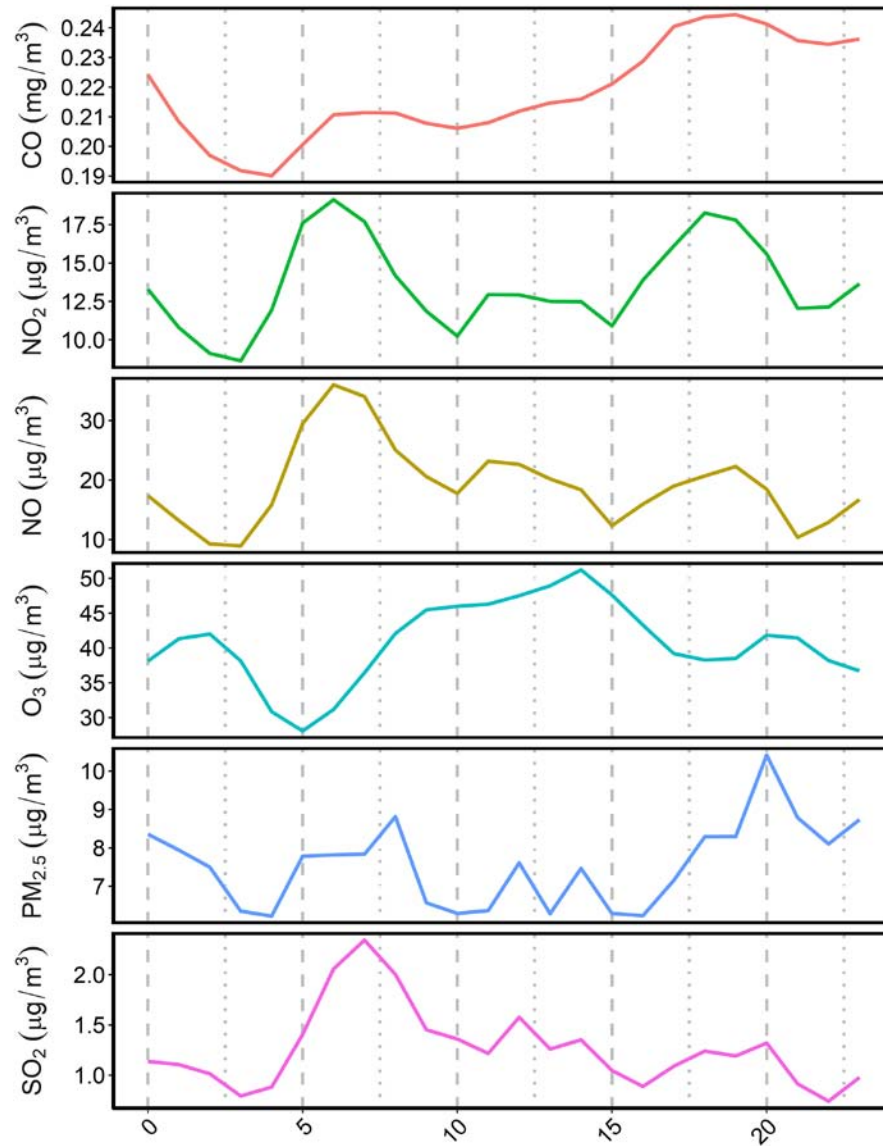


Figure 3.2. Diurnal profiles for the main pollutants measured at the PortAIR measurement site during 2022.

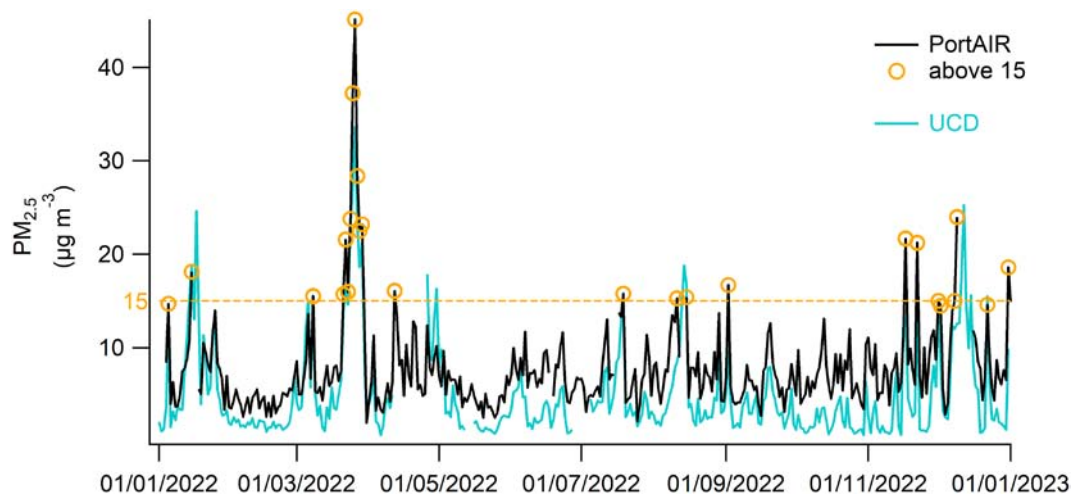


Figure 3.3. Daily average reconstructed $\text{PM}_{2.5}$ mass concentration ($\text{PM}_{\text{acsm+eBC}}$) at the PortAIR and UCD monitoring sites for 2022. Markers indicate days where the average daily $\text{PM}_{2.5}$ concentration at the PortAIR site was above the WHO recommended 24-hour AQG value of $15 \mu\text{g m}^{-3}$.

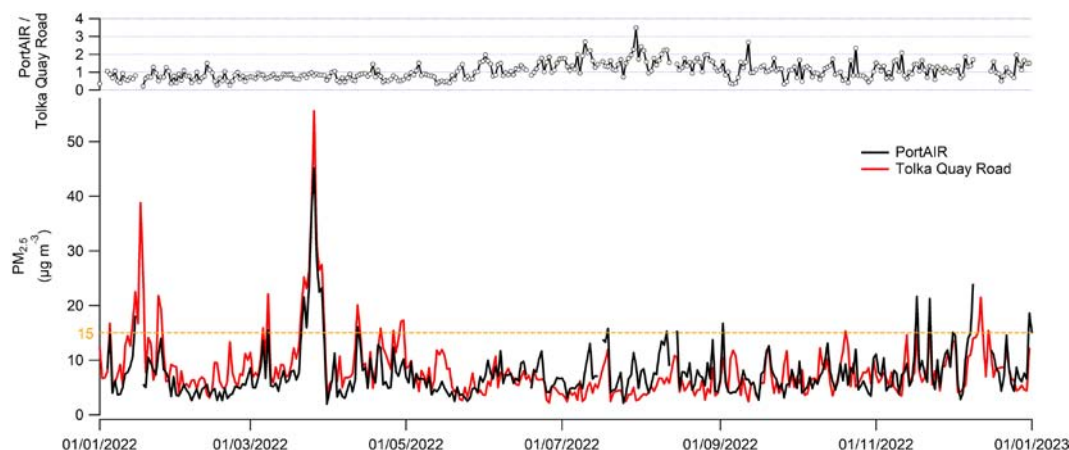


Figure 3.4. Daily $PM_{2.5}$ concentrations from the PortAIR (reconstructed in black) and Tolka Quay Road (Station 76, “Dublin Port”) sites. The ratio of $PM_{2.5}$ concentrations (PortAIR/Tolka Quay Road) is shown in the top panel.

and measurement technique, with the annual mean concentrations of $PM_{2.5}$ within 10% of each other.

3.2 Air Sensor Network

A summary of the $PM_{2.5}$ data collected by each of the air sensors is presented in Table 3.2. The mean $PM_{2.5}$ concentration observed by all sensors is in a similar range, between 4.5 and 6.5 $\mu g m^{-3}$, with the two sensors located at the PortAIR site showing some of the highest mean concentrations. Multiple sensors measured $PM_{2.5}$ concentrations above 100 $\mu g m^{-3}$ throughout the campaign, with the most intense spike (137 $\mu g m^{-3}$) observed at the Ringsend site, which is a roadside location close to a residential area. There is good consistency between the concentrations observed across the sensor network,

with differences between locations likely to be due to variations in emissions from traffic and other hyperlocal sources. Overall, the data are of good quality, highlighting the potential for use of sensor networks in highly dynamic environments.

The corrected $PM_{2.5}$ data from sensor ANG5-000279 located at the PortAIR site were compared with the reconstructed $PM_{2.5}$ data (Figure 3.5). There is good correlation between the two datasets, with similar spikes in concentration observed by both instruments; however, it is noted that the sensor still under-reported $PM_{2.5}$ concentration by around 20% compared with the reconstructed mass. Nevertheless, these data highlight the promising outlook for the use of a low-cost sensor network to monitor particulate pollution in the port area.

Table 3.2. Summary statistics for $PM_{2.5}$ measurements (corrected data) in the air sensor network during the measurement campaign

| Sensor name | Location | Mean $PM_{2.5}$ ($\mu g m^{-3}$) | Median $PM_{2.5}$ ($\mu g m^{-3}$) | Maximum $PM_{2.5}$ ($\mu g m^{-3}$) | Minimum $PM_{2.5}$ ($\mu g m^{-3}$) | Data capture (%) |
|-------------|--------------------------|------------------------------------|--------------------------------------|---------------------------------------|---------------------------------------|------------------|
| ANG5-00244 | Promenade Road | 6.17 | 4.34 | 112.02 | 0.21 | 90.21 |
| ANG5-00260 | Dublin Port (Station 76) | 5.62 | 4.02 | 94.82 | 0.32 | 99.26 |
| ANG5-00263 | Irish Ferries | 5.90 | 4.47 | 119.64 | 0.30 | 91.35 |
| ANG5-00266 | DPC headquarters | 4.85 | 3.27 | 30.97 | 0.18 | 17.13* |
| ANG5-00268 | North Wall Quay | 5.54 | 3.86 | 112.77 | 0.18 | 99.31 |
| ANG5-00269 | PortAIR site | 5.79 | 4.31 | 73.80 | 0.41 | 81.61 |
| ANG5-00275 | Poolbeg | 4.73 | 3.18 | 42.90 | 0.18 | 36.05* |
| ANG5-00277 | Ringsend (Station 17) | 4.67 | 3.17 | 137.34 | 0.14 | 99.24 |
| ANG5-00279 | PortAIR site | 6.12 | 4.49 | 127.22 | 0.34 | 99.31 |

*Low data capture percentage due to recurring power failure at these sites.

DPC, Dublin Port Company.

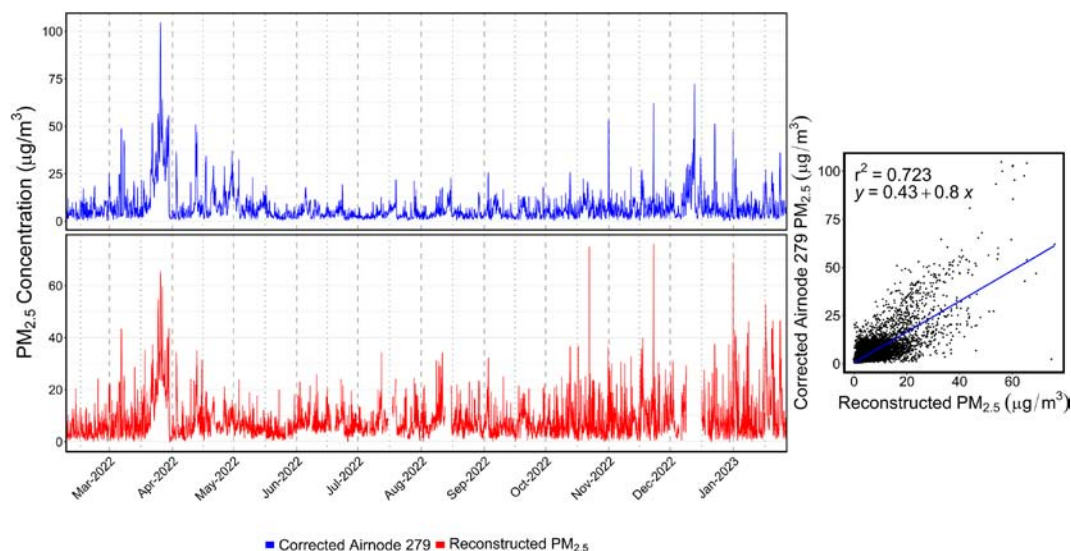


Figure 3.5. Comparison of $\text{PM}_{2.5}$ concentrations obtained using an air sensor (AirNode 279, Airscape) with the reconstructed mass determined from the Q-ACSM+eBC data at the PortAIR site.

3.3 Mean $\text{PM}_{2.5}$ Chemical Composition for 2022

3.3.1 Online analysis (Q-ACSM and equivalent black carbon)

The online particle composition data for 2022 are shown in Figure 3.6 as daily (midnight–midnight) concentrations of reconstructed $\text{PM}_{2.5}$. Carbonaceous aerosol (OA+eBC) constituted at least 69% of the reconstructed $\text{PM}_{2.5}$. However, inorganic species (NO_3^- , SO_4^{2-} and NH_4^+ , predominantly) occasionally

accounted for a much larger fraction, such as during the regional pollution event from 21 March 2022 to 30 March 2022. Overall, $\text{PM}_{2.5}$ was composed of 50% OA, 19% eBC, 16% SO_4^{2-} , 9% NO_3^- , 5% NH_4^+ and 1% Cl^- . There was comparatively more OA and eBC at the PortAIR site than at the urban background site at UCD (Figure 3.7), which points to more local sources of both species in the Dublin Port area. While eBC makes up a high accumulative fraction of the yearly data, maximum eBC concentrations reached only $20 \mu\text{g m}^{-3}$, compared with SO_4^{2-} that reached $65 \mu\text{g m}^{-3}$ and NO_3^- that reached $36 \mu\text{g m}^{-3}$ (Table 3.3).

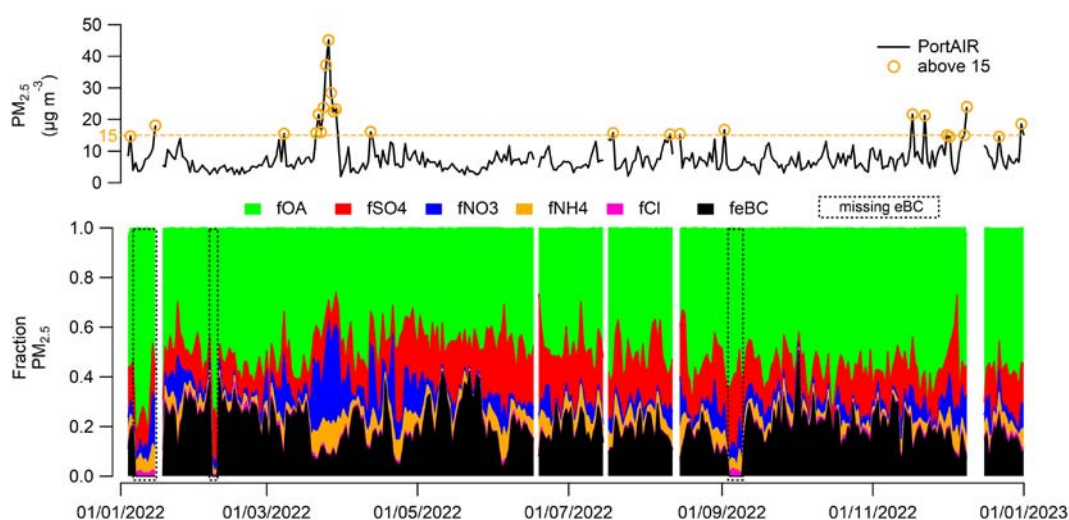


Figure 3.6. Daily $\text{PM}_{2.5}$ concentrations at the PortAIR site (reconstructed in black). Markers indicate days when the daily concentration was above the WHO AQG value (top). A time series of the relative fraction (f) of aerosol species from the ACSM (OA, SO_4 , NO_3 , NH_4 , Cl) and AE33 (eBC) contributing to the daily $\text{PM}_{2.5}$ concentrations (bottom).

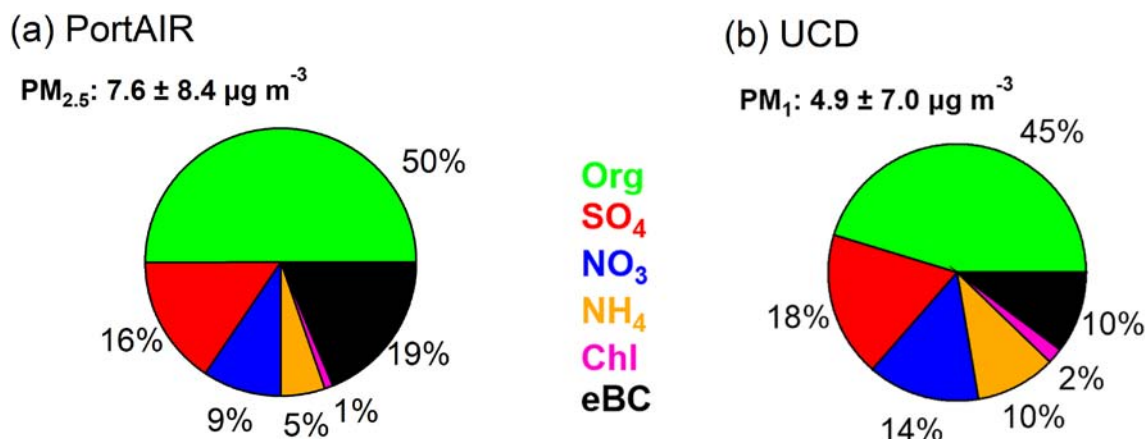


Figure 3.7. A pie chart of the average species contribution (%) for 2022 is shown for (a) PortAIR and (b) UCD.

Table 3.3. Summary statistics for the concentration of $PM_{2.5}$ chemical components (expressed in $\mu g m^{-3}$) derived from online analysis using ACSM and eBC

| Species | Average | Standard deviation | Minimum | Maximum |
|-------------|---------|--------------------|---------|---------|
| OA | 3.8 | 5.7 | BDL | 141 |
| eBC | 1.4 | 1.4 | BDL | 20 |
| SO_4^{2-} | 1.2 | 1.6 | BDL | 65 |
| NO_3^- | 0.7 | 1.9 | BDL | 36 |
| NH_4^+ | 0.4 | 1.3 | BDL | 11 |
| Cl^- | 0.08 | 0.18 | BDL | 6 |

Minimum values are defined as below the detection limit (BDL) of the instruments.

3.3.2 Offline analysis (X-ray fluorescence and organic carbon–elemental carbon)

Table 3.4 shows the summary statistics for the ambient concentrations of inorganic elements, as well as OC and EC from the filter collections, for the entire year 2022. Several samples produced concentrations that were below the method detection limits, and so the percentage BDL (below detection limit) for each species is included in the table. In samples where concentrations were analytically below the detection limits for the respective species, it could not be assumed that they were zero, and so the analytical value was replaced with half the detection limit and the average was calculated from all samples, including the BDL samples (set equal to $0.5 \times BDL$). For species that were below the detection limit in any samples, the minimum values in the table represent the detection limit.

As expected, the total OA and SO_4^{2-} measured by the Q-ACSM shows good correlation with filter-based

measurements of OC ($r_{\text{Pearson}} = 0.79$) and sulfur ($r_{\text{Pearson}} = 0.7$), respectively. Concentrations of NO_3^- and NH_4^+ provided by the Q-ACSM are also highly correlated with the filter-based sulfur measurements, indicating that these species are likely to be related to the secondary inorganic aerosol species, ammonium nitrate and ammonium sulfate. There is also a strong correlation throughout the year between V and Ni as common ship emission marker species.

However, it is worth noting that the correlation between Cl^- measured online by the Q-ACSM shows no correlation with the concentrations determined from filter collections ($r_{\text{Pearson}} = -0.04$). In general terms, the sources identified by the Q-ACSM data can include only organic species and the major ions NH_4^+ , NO_3^- and SO_4^{2-} , and so the additional chemical species obtained by offline elemental analysis can help determine the influence of sources characterised by mineral species, like road dust, sea salt and crustal material. However, as will be shown below,

Table 3.4. Summary statistics for the concentration of PM_{2.5} chemical components (expressed in ng m⁻³) derived from offline analysis using XRF and the OC–EC analyser

| Species | Mean | Standard deviation | Minimum | Maximum | % BDL |
|---------|-------|--------------------|---------|---------|-------|
| OC | 1.872 | 1.769 | 0.727 | 10.356 | 0.0 |
| EC | 0.882 | 0.528 | 0.142 | 4.198 | 0.0 |
| Na | 0.513 | 0.925 | 0.519 | 3.005 | 51.3 |
| Mg | 0.413 | 0.069 | 0.320 | 0.526 | 99.8 |
| S | 0.264 | 0.141 | 0.076 | 0.935 | 0.0 |
| Cl | 0.148 | 0.216 | 0.001 | 1.221 | 16.7 |
| Ca | 0.034 | 0.027 | 0.018 | 0.178 | 1.1 |
| K | 0.033 | 0.044 | 0.005 | 0.602 | 0.0 |
| Fe | 0.020 | 0.016 | 0.004 | 0.112 | 5.4 |
| Ba | 0.014 | 0.027 | 0.228 | 0.327 | 46.8 |
| V | 0.005 | 0.010 | 0.008 | 0.063 | 39.9 |
| Zn | 0.004 | 0.005 | 0.003 | 0.024 | 46.4 |
| Ti | 0.003 | 0.005 | 0.009 | 0.017 | 76.4 |
| Ni | 0.003 | 0.004 | 0.003 | 0.019 | 51.1 |
| Br | 0.002 | 0.004 | 0.005 | 0.024 | 61.8 |
| Pb | 0.001 | 0.002 | 0.009 | 0.010 | 73.8 |
| Cu | 0.001 | 0.001 | 0.003 | 0.013 | 77.3 |
| Mn | 0.000 | 0.001 | 0.005 | 0.002 | 78.1 |
| Cr | 0.000 | 0.001 | 0.007 | 0.003 | 77.9 |

the inorganic speciation alone could lead to some important ship emissions being missed entirely because the common ship emission marker species V and Ni cannot be used to unequivocally identify ships using low-sulfur fuels.

3.4 Characterisation of Ship Emissions During the Intensive Measurement Period

The Q-ASCM and Xact instruments were combined during the intensive measurement period to enable a more detailed analysis of the chemical composition of ship plumes. Shipping logs and information from shipping companies on the types of fuel used in their vessels were used to interpret the chemical data. Under the EU Sulphur Directive, ships at berth in Dublin Port are required to use ULSFO while at berth or else implement the use of scrubbers aboard the ship to reduce SO₂ emissions from burning fuels with higher sulfur content. The permissible fuel use behaviours at Dublin Port were (i) using ULSFOs only (mainly marine gas oil (MGO)), (ii) using VLSFO to power the engines and MGO for electricity generators when in port, (iii) using HFO for engines (with a

scrubber) and MGO for generators when in port, and (iv) using HFO with a wet scrubber operated using a closed-loop system all the time.

An overview of the high time resolution measurements from the intensive period is shown in Figure 3.8. Many high-pollution events of short duration were observed, with the peak PM₁ mass concentration reaching 252 µg m⁻³. The pollution events typically lasted 5–35 minutes and were driven by OA, often in combination with SO₄²⁻ and other inorganic species. Elemental sulfur, V and Ni were also present during pollution plumes that contained SO₄²⁻. While the V/Ni ratio was often in the range 2.5–4.0, consistent with HFO emissions (Pandolfi *et al.*, 2011; Viana *et al.*, 2009), an appreciable number of pollution spikes occurred when the V/Ni ratio was less than 2.5, suggesting that they are not attributable to HFO emissions. The spikes in PM₁ occurred in conjunction with increased SO₂ and NO_x concentrations, and enhanced aerosol number concentration ($d_p = 10\text{--}500\text{ nm}$). However, enhanced number concentration did not always result in very high mass concentrations of the aerosol, as they were driven by smaller diameter aerosol particles (Fossum *et al.*, 2024). The very local nature of these pollution spikes

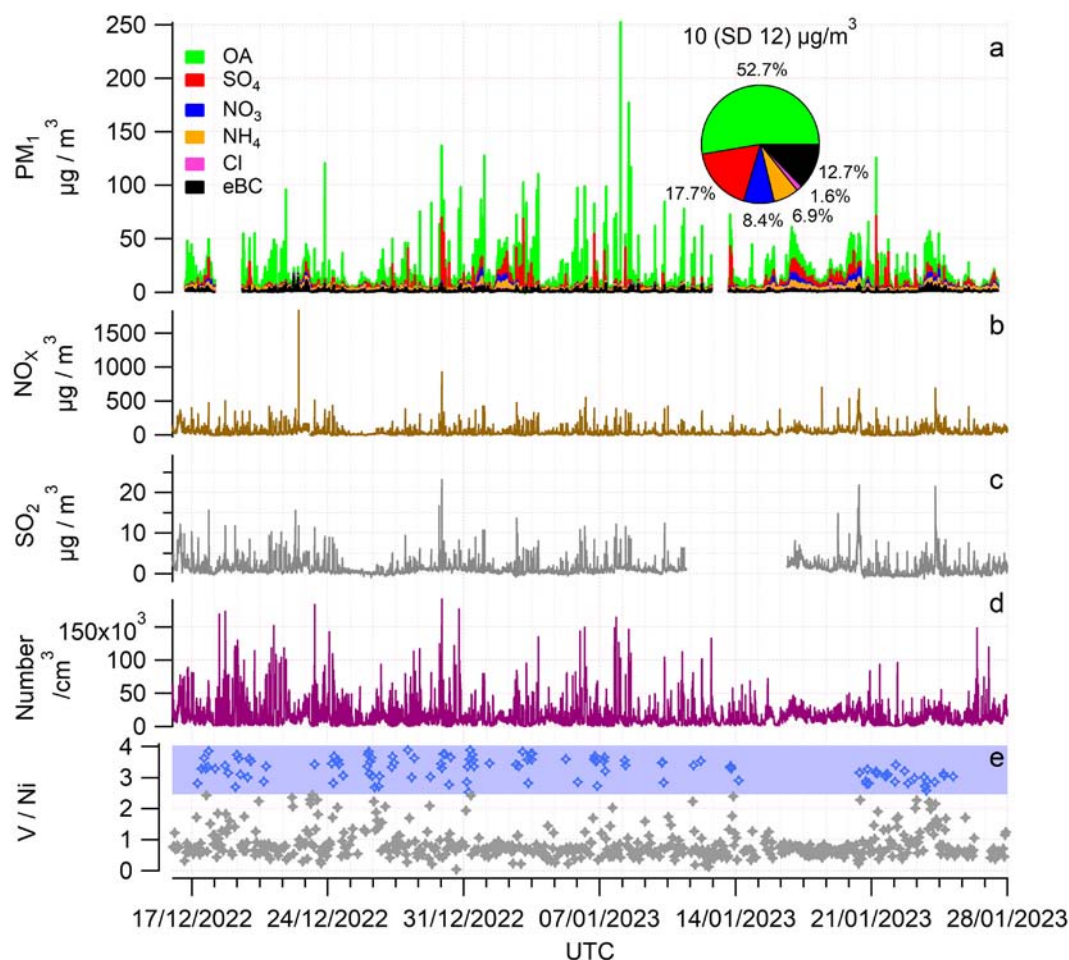


Figure 3.8. Time series of the high time resolution ambient measurements during the intensive PortAIR campaign. (a) Reconstructed PM_{10} on the left axis formed from stacked species along with a pie chart of the average contributions of each (mean PM_{10} (standard deviation) is shown above the pie chart); (b) NO_x in brown; (c) SO_2 in grey; (d) particle number concentration from 10 to 500 nm in dry electrical mobility diameter (d_m) from the SMPS; and (e) V/N ratio as measured by the Xact, with the blue shaded area denoting the range of V/Ni traditionally associated with HFO and blue markers showing data in the range (grey when not).

is verified by comparing the results with those obtained at the urban background site at UCD. The comparison shows that while most regional pollution events occur simultaneously at both sites, Dublin Port also has unique and localised pollution spikes that do not occur at the UCD site. Thus, source apportionment modelling was used to explore and identify the origins of these short-lived pollution episodes.

3.4.1 Ship profile identification

To derive a ship emission profile, time series data were used to search for short-lived pollution events, with known markers, including V/Ni ratios, SO_2 and NO_x concurrent spikes, and OA with a mass spectral

profile, indicative of oil or petrol fuel burning. Since the Xact was measuring at hourly time resolution, the V and Ni data were treated as an indicator of a shipping emission plume within that hour. The presence of concurrent spikes in the higher time resolution SO_2 and NO_x data was subsequently used to determine the time and duration of likely shipping plumes. Using the markers, around 50 plumes were manually identified with a V/Ni ratio in the expected range for HFO emissions and these plumes occurred when the wind direction was primarily from the south (south-west to south-east included), inferring advection of plumes from nearby ferry berths, the marine shipping channel and South Dublin Port. However, there were many OA-dominated plumes that lacked V

and Ni in either significant concentrations or when the ratio was lower than the expected range for HFO. In these cases, the OA-dominated plumes still contained concurrent spikes in SO_2 and NO_x concentrations and occurred when the wind direction came from the south-western side of the port across a nearby ferry berth or at times when ships were either in the process of docking or docked. Since the classical V/Ni ratio may no longer be a reliable marker for emissions from ships using low-sulfur marine fuels, the results obtained here were used to categorise two different types of ship plumes as follows:

S-Ship. Sulfate-rich ship emissions that are characterised by elevated V ($0.55\text{--}0.17\text{ }\mu\text{g m}^{-3}$) and Ni ($0.16\text{--}0.05\text{ }\mu\text{g m}^{-3}$) concentrations and have the well-documented V/Ni ratio of 2.5–4.0 associated with HFO, high elemental sulfur concentrations, and elevated SO_2 and NO_x concentrations. These pollution spikes are also associated with significant concentrations of particulate SO_4^{2-} relative to OA.

O-Ship. Organic-rich ship emissions that are dominated by OA and have elevated SO_2 and NO_x concentrations, but do not have the V/Ni ratio

associated with HFO and have significantly lower V ($<0.04\text{ }\mu\text{g m}^{-3}$) and Ni ($<0.02\text{ }\mu\text{g m}^{-3}$) concentrations.

To derive the Q-ACSM mass spectral signatures for S-Ship and O-Ship, five exemplary plumes of each type were selected for detailed analysis. Due to the high SO_4^{2-} content in the plumes, it was necessary to implement a combined SO_4^{2-} –OA component PMF of the ACSM data, rather than the traditional OA PMF. The PMF analysis used Q-ACSM mass spectral signatures derived for O-Ship and S-Ship along with signatures for other expected sources, such as traffic hydrocarbon-like organic aerosol (HOA) obtained from a previous roadside study in Dublin, Ireland, as well as individual solid fuel burning factors for peat, wood and coal from another previous Irish study, and a sea salt profile. A six-factor solution was obtained, comprising four constrained factors (S-Ship, O-Ship, HOA, peat) and two unconstrained factors (oxygenated organic aerosol (OOA) and a minor ship factor, X-Ship) (Figure 3.9). This second unconstrained factor (X-Ship) has a time series that is well correlated with O-Ship and to a lesser extent with HOA and S-Ship. Due to association with both shipping factors,

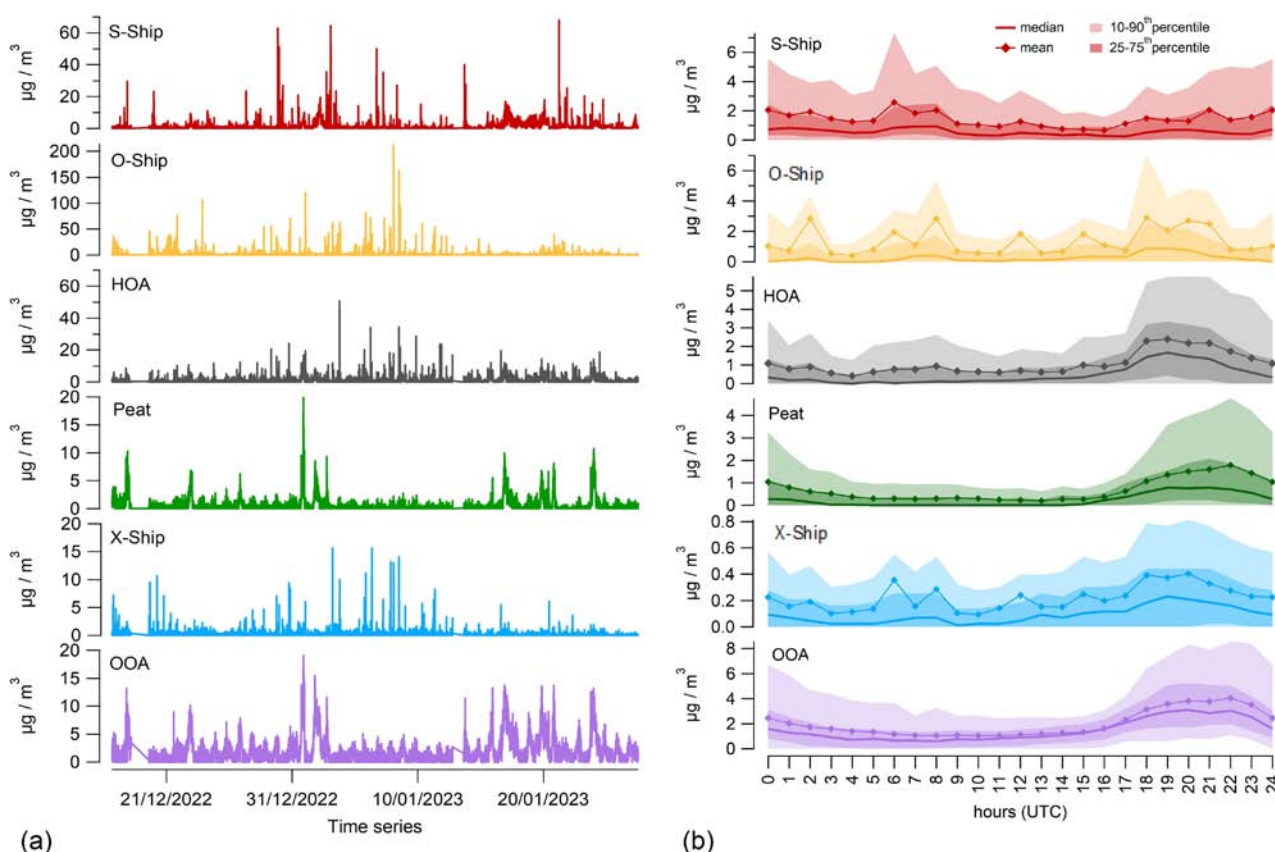


Figure 3.9. The six-factor PMF solution showing the time series (a) and the diurnal profiles (b).

this factor points to a source related to ship engines, mostly to vessels using low-sulfur fuels (for more details see Fossum *et al.*, 2024).

The PMF analysis identified a total of 58 S-Ship plumes and 190 O-Ship plumes during the intensive measurement campaign. The mean characteristics of the ship plumes are summarised in Table 3.5.

The average chemical breakdown of PM_{10} , along with NO_x and SO_2 , is shown in Figure 3.10a for S-Ship and in Figure 3.10b for O-Ship. The S-Ship factor plumes comprised mostly SO_4^{2-} (57%), followed by OA (35%), eBC (6%) and NO_3^- (1%), with negligible contributions from NH_4^+ and Cl^- . O-Ship plumes comprised mostly OA (77%), followed by eBC (9%), SO_4^{2-} (7%), NO_3^- (3%), NH_4^+ (3%) and Cl^- (1%).

Close investigation of the factors, combined with information on vessel fuel use, wind direction and shipping logs, confirms that the S-Ship plumes originate from vessels using HFO (sulfur content <3.5% m/m) with a scrubber system to remove gaseous SO_2 emissions, while O-Ship plumes originate from vessels that use VLSFO (sulfur content <0.5% m/m). Referring to Table 3.5, it is interesting to note that the scrubbed HFO emissions have slightly lower NO_x , SO_2 , and particulate mass and number

concentrations than VLSFO. However, the scrubbed HFO emissions are acidic (contain SO_4^{2-}) and contain higher heavy metal concentrations than VLSFO.

3.4.2 Q-ACSM source apportionment

Factors from the OA- SO_4^{2-} PMF, inorganic species and eBC were combined to obtain a composition breakdown of the measured PM_{10} (Figure 3.11a). To transform the various factors and eBC into more complete representations of source contributions, regional SO_4^{2-} had to be subtracted from S-Ship SO_4^{2-} and eBC needed to be attributed to both the ship emissions, as the expected ratios of eBC/OA for these plumes were measured *in situ*. The resulting source contribution estimates were labelled O-Ship*, S-Ship* and eBC*, in order for them not to be confused with previous factors, and measured total eBC. Factors and chemical components that belong to regional sources, which include OOA, NO_3^- , NH_4^+ , Cl^- and regional SO_4^{2-} subtracted from S-Ship, were combined into one regional source category.

Across the campaign, the source contributions to the measured PM_{10} were regional (46%), O-Ship* emissions (14%), S-Ship* emissions (12%), HOA due to traffic or oil burning (10%), eBC* (9%), peat (6%)

Table 3.5. Mean characteristics of S-Ship and O-Ship plumes detected during the intensive measurement campaign

| Plume type | No. of plumes | PM_{10} ($\mu g m^{-3}$) | N ($/cm^{-3}$) | NO_x ($\mu g m^{-3}$) | SO_2 ($\mu g m^{-3}$) | eBC ($\mu g m^{-3}$) | V/Ni | V ($\mu g m^{-3}$) | N ($\mu g m^{-3}$) |
|------------|---------------|------------------------------|-------------------------------|---------------------------|---------------------------|------------------------|-----------|----------------------------|----------------------------|
| S-Ship | 58 | 29±22 | $(1.52 \pm 1.55) \times 10^4$ | 117.6±118.0 | 3.5±3.4 | 1.8±1.4 | 3.41±0.28 | 0.21±0.15 | 0.060±0.042 |
| O-Ship | 190 | 32±26 | $(3.75 \pm 2.28) \times 10^4$ | 132.3±108.7 | 3.9±3.2 | 3.0±1.8 | 0.74±0.35 | $(7 \pm 6) \times 10^{-3}$ | $(8 \pm 7) \times 10^{-3}$ |

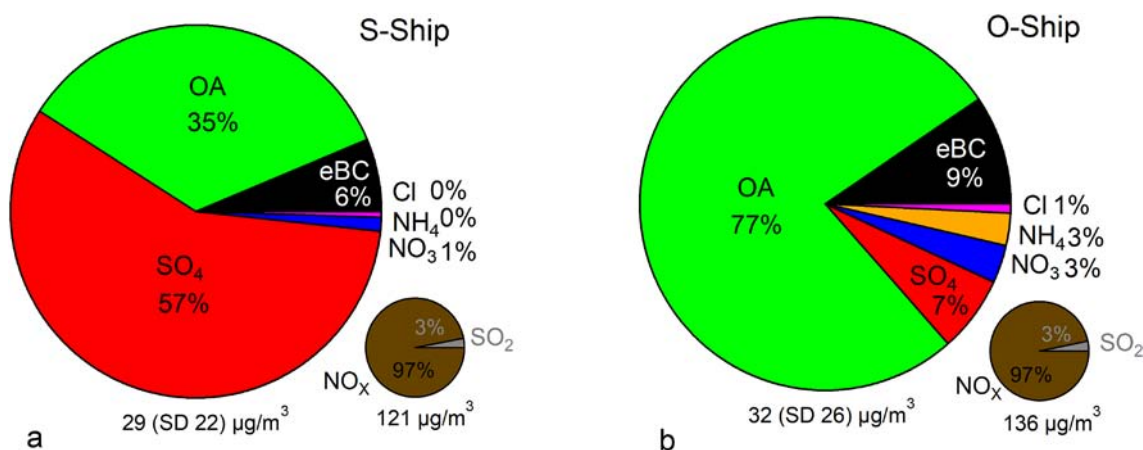


Figure 3.10. Pie charts of the composition breakdown of PM_{10} for S-Ship plumes (a) and O-Ship plumes (b), with gas data pie charts for SO_2 and NO_x also shown.

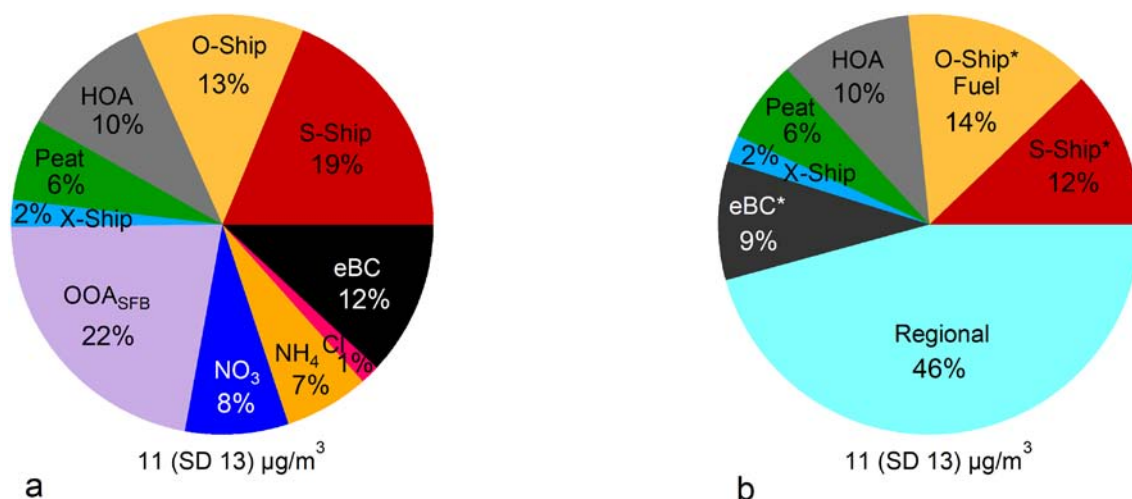


Figure 3.11. Pie charts showing the PMF factors and other species contributing to PM_1 (a) and source contribution estimates to PM_1 with adjusted O-Ship, S-Ship and eBC (b). Mean PM_1 is shown at the bottom of the pie charts (with the standard deviation of the mean in brackets).

and X-Ship emissions (2%). The Dublin Port ship emissions made up 28% (S-Ship*, O-Ship* and X-Ship) of PM_1 , and did not include ship traffic-related HOA and associated port traffic and shipping lane eBC. It was difficult to attribute the HOA factor in Dublin Port to either ship-related traffic, city traffic or oil burning for residential heating, as the pollution roses indicate only a local and often westerly source. Therefore, we estimate that shipping-related emissions at the PortAIR site contributed 28–47% of PM_1 (Figure 3.11b), as some significant portion of the HOA and traffic-related eBC was expected to come

from sources such as ferry traffic, vehicles for moving containers and crane engines.

3.4.3 Xact source apportionment

The factor contribution profiles obtained from PMF analysis performed on the Xact data are given in Figure 3.12. Four factors were identified, with Factor 1 having almost all the chlorine, Factor 2 containing most of the As, Ba and Se, Factor 3 having the dominant amount of V and Ni, and Factor 4 containing a wide range of elements.

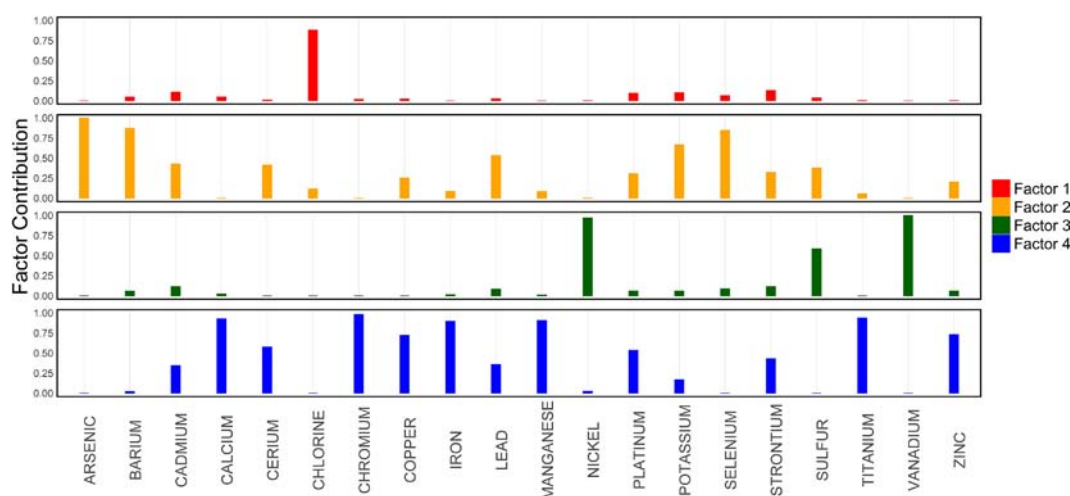


Figure 3.12. Factor contribution profiles for the chosen four-factor solution from the Xact 625i PMF analysis. The y-axis represents the fraction of each metal apportioned to a given factor, for example the Ni and V fractions in Factor 3 are c.1.00, meaning that close to 100% of Ni and V appears in Factor 3.

The factor profiles provide some information in isolation, notably the prevalence of V and Ni in Factor 3 indicative of HFO emissions; however, interpretation of the temporal and diurnal profiles in Figures 3.13 and 3.14, respectively, allows the sources contributing to each factor to be further elucidated.

The diurnal and temporal profiles provide further information and allow the factors to be classified as (i) background, (ii) residential solid fuel burning, (iii) HFO from shipping and (iv) daytime activities. Interpreting these time series with the factor profiles

outlined in Figure 3.12 provides further evidence for their assignment. Factor 1 is dominant in chlorine, suggesting sea salt as a possible source, although this would need to be confirmed through detection of Na. The strong contribution from As and K to Factor 2 supports the assignment of residential solid fuel burning as the source, since both elements are consistently found in coal and wood, respectively. As previously mentioned, V and Ni are widely known markers for HFO, which is used in marine environments, explaining their prevalence in Factor 3, while the presence of sulfur in both Factor 2 and

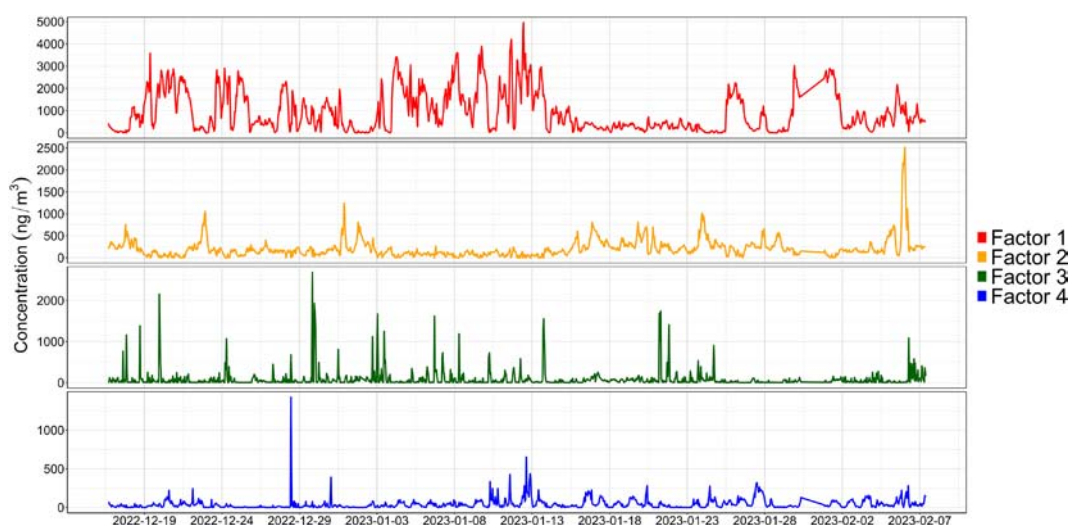


Figure 3.13. Time series for the four factors obtained from PMF analysis performed on the Xact data.

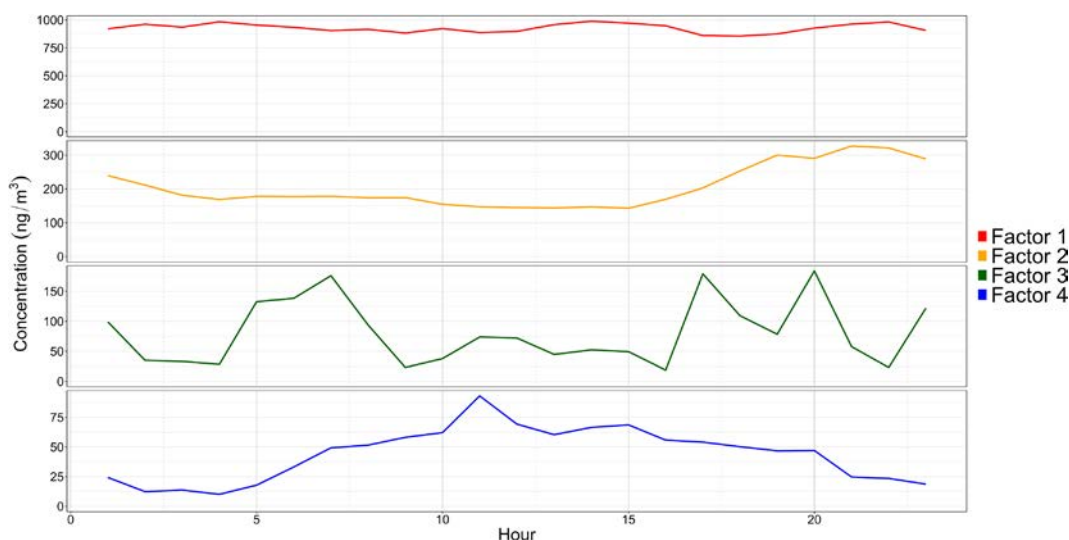


Figure 3.14. Diurnal profiles for the four factors obtained from PMF analysis performed on the Xact data. Factor 1 shows little to no diurnal variability, suggesting that it is a background factor; Factor 2 shows a strong evening peak, which may highlight a contribution from residential solid fuel burning; Factor 3 shows a very similar trend to ship emissions; and Factor 4 has a strong daytime contribution, suggesting that it is related to in-port activities such as construction.

Factor 3 is a strong indicator that these factors are related to fuel combustion processes. Factor 4, meanwhile, has a strong contribution from elements such as Ca, Mn, Fe and Zn. These are markers for crustal elements, possibly resuspended during the construction and transport works undertaken throughout the port. Other elements in this factor could be due to emissions from vehicle brake and tyre wear. The broad daytime peak observed for this factor is indicative of in-port emissions and activities, but could also contain contributions from Dublin city centre.

The PMF factors derived from analysis of the Xact and Q-ACSM data were compared, with the results represented in the form of a correlation matrix (Figure 3.15).

Factor 1 correlates reasonably well with O_3 , which is a good indicator that this is a regional factor and could be related to long-range transport. Factor 2 correlates with numerous typical components of residential solid fuel burning, including black carbon and CO , as well as the Q-ACSM factors HOA, peat and OOA. Factor 3 correlates well with the S-Ship

factor; however, it does not correlate well with either the O-Ship or X-Ship factors, again supporting the assignment of this factor to HFO emissions. Interestingly, Factor 4 correlates with no other variable in the matrix, indicating that this is a new factor that is not associated with substantial OA and is therefore unaccounted for by the Q-ACSM PMF analysis. Further interrogation of additional data, such as particle size and number concentrations, could help to elucidate the source of this factor.

3.4.4 Ship emissions when manoeuvring and hoteling

In Dublin Port, ship manoeuvring takes on average 30 ± 10 minutes from the outer buoy to docking. Additionally, there is no shore-side electricity, and so the ships run their engines or generators when at dock, a process called “hoteling”. The emissions from ships are expected to be different during manoeuvring because the engine is under a different load compared with hoteling or cruising, and also ships may switch to different engines with compliant fuels (for a Sulfur

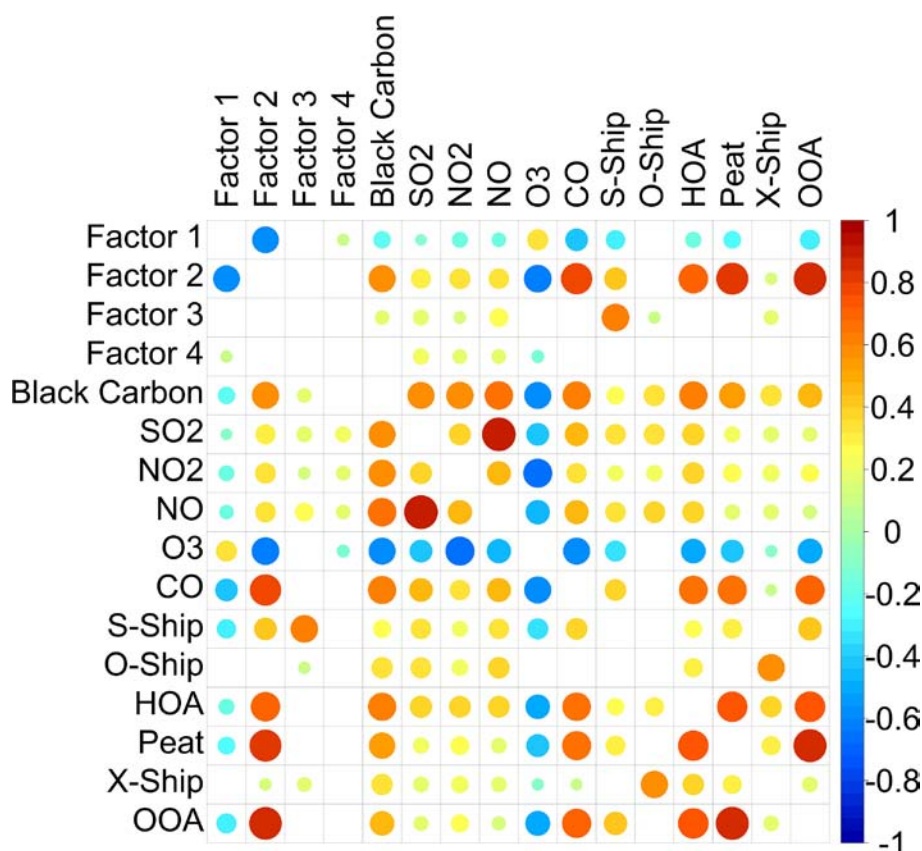


Figure 3.15. Correlation matrix comparing the Xact PMF factors with other pollutants and the ACSM-derived PMF factors during the intensive measurement campaign.

Emission Control Area) after docking. Thus, it was interesting to note that, when meteorological conditions were steady, the manoeuvring in and out of the nearby berths showed distinct plumes with hoteling periods in between, resulting in time series of both mass and number concentration that resembled the shape of bat ears (Figure 3.16). The “bat ear” profiles are characterised by intense plumes of PM_{10} , NO_x and SO_2 during inbound and outbound manoeuvring, with a large drop in concentration in between, where PM_{10} typically fell below $15 \mu\text{g m}^{-3}$ and the gas concentrations also dropped but remained elevated above background concentrations. This drop in PM_{10} is partially an artefact of the sampling technique used by the ACSM, which has a lower particle size cut-off of roughly 40 nm vacuum aerodynamic diameter (equivalent to $\sim 32 \text{ nm}$ electrical mobility diameter).

The O-Ship “bat ear” profiles shown in Figure 3.16 are the result of VLSFO-powered vessels switching to MGO when docked. While not as visible in the Q-ACSM sampled mass concentration, MGO emissions are visible in the number–size distribution as large concentrations (e.g. $6 \times 10^4 \text{ cm}^{-3}$) of tiny particles with $d_m < 50 \text{ nm}$. The hoteling periods are

characterised by particles with $d_m < 32 \text{ nm}$, contributing 51–100% of the estimated SMPS particle volume, which is smaller than the lower cut-off size of the aerodynamic lens in the Q-ACSM. This means that a significant portion of MGO particle emissions is not captured by the Q-ACSM and does not contribute to the reconstructed PM_{10} mass concentration or source contribution estimates shown in Figure 3.10. It is important to note that this limitation is not restricted to the Q-ACSM, because many other instruments, including the reference PM monitors that use optical light scattering, e.g. the Fidas instruments used in the ambient air quality monitoring network, do not detect particles in the low tens of nm size range. Nonetheless, estimates of the mass concentration during the four hoteling periods (in chronological order) have been determined from the SMPS data (assuming spherical OA particles with a density of 1.27 g cm^{-3} to be 11, 30, 15 and $54 \mu\text{g m}^{-3}$, respectively) (Fossum *et al.*, 2024). Overall, these time profiles confirm that ship emissions from vessels during hoteling yield concentrations of particles that are shifted to smaller sizes, which may be missed in PM_{10} and $\text{PM}_{2.5}$ estimates.

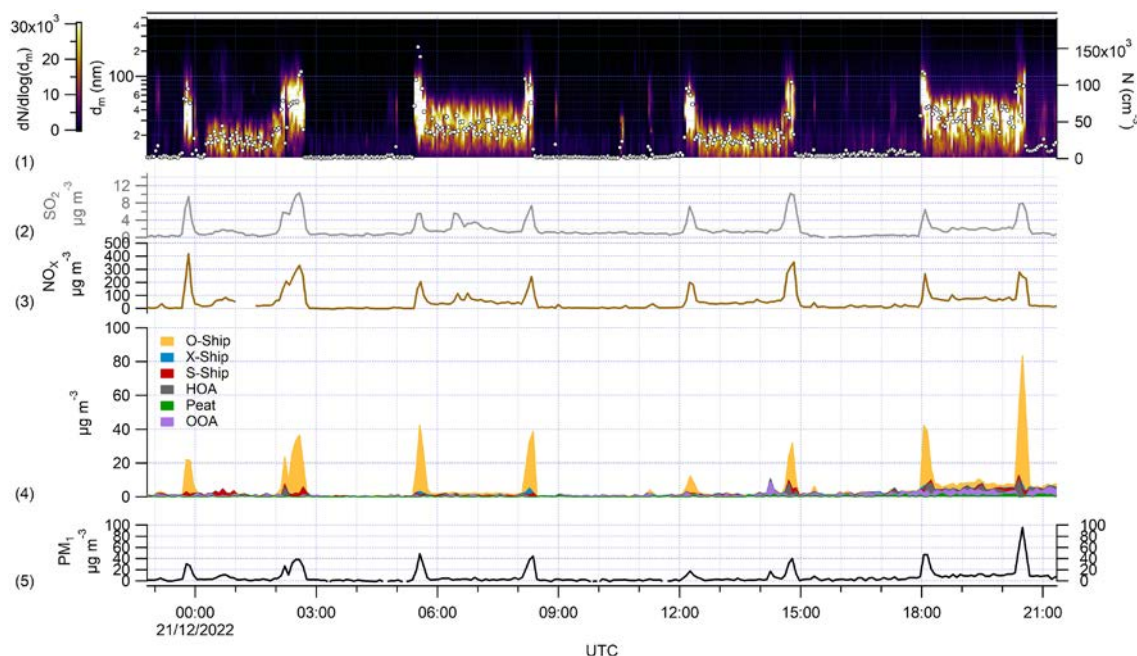


Figure 3.16. Time series of data during “bat ear” ship emission events for isolated O-Ship plumes (fuel switching pattern VLSFO–MGO–VLSFO). Panel (1) shows a curtain plot of particle number–size distribution data with particle diameter (d_m (nm)) (left axis) and lognormal particle concentration ($dN/d\log(d_m)$) indicated by colour, while the particle number concentration (cm^{-3}) is shown as white circles (right axis). Panel (2) shows SO_2 data (grey); panel (3) shows NO_x data (brown); panel (4) shows PMF factors (as in Figure 3.9); and panel (5) shows PM_{10} .

3.5 PM_{2.5} Source Apportionment for 2022

Source apportionment of PM_{2.5} was conducted for the period 1 January to 31 December 2022 using the continuously collected Q-ACSM data. In principle, the information obtained from offline analysis of 24-hour filter samples could supplement the analysis; however, many of the elements were observed at concentrations below the detection limits, and including these data in a receptor model would lead to higher uncertainties in the source contribution estimates.

3.5.1 Online analysis (Q-ACSM and equivalent black carbon)

PMF was performed using the protocol established from the intensive measurement period. Briefly, the factors for S-Ship, O-Ship, HOA, peat and X-Ship were used to constrain the model on a seasonal basis using 5-minute resolution data on combined OA–SO₄²⁻ Q-ACSM data. One main difference from the intensive period was that X-Ship was constrained, as a variation on this factor would emerge from the free PMF but only above seven free factors. Another difference was that the pass limits approach was used with altered parameters for S-Ship, O-Ship and HOA, based on differences between the fragmentation patterns obtained using the PM₁ Q-ACSM during the intensive campaign and the PM_{2.5} Q-ACSM from the rest of 2022 (1 January to 9 December 2022). The peat factor pass

limits remained the same, and a constant α -value of 0.05 was used for constraining the X-Ship profile. This α -value was found through sensitivity testing.

A seven-factor solution was chosen, in contrast to the intensive campaign that had a six-factor solution. The additional factor in the seven-factor solution for the year-long data comes from the separation of SO₄²⁻ from the OOA factor, which was found in the intensive campaign. In the year-long dataset, a seventh regional SO₄²⁻ factor, comprising almost entirely SO₄²⁻ ions, emerges. In Figure 3.17, the OOA and SO₄²⁻ factors have been combined into one factor named OOA+ to make it comparable with the intensive period.

Figure 3.17 shows the monthly contributions of the various PMF factors in 2022. Overall, the contribution of combined ship-related factors (S-Ship, O-Ship and X-Ship) is in the range of 20–30% of the OA–SO₄²⁻ mass. Figure 3.13c shows the sources resolved from the combination of PMF factors from OA–SO₄²⁻ in combination with the other species. The procedure for the quantification of the sources is identical to that described in section 3.3.2 (see Figure 3.11b). Factors and chemical components that belong to regional sources, which includes OOA+, NO₃⁻, NH₄⁺ and Cl⁻, were combined into one regional source. Overall, the 2022 PM_{2.5} breakdown shows 56% regional contribution, 15% eBC, 11% S-Ship, 7% O-Ship, 6% HOA, 4% peat and 3% X-Ship. The ship-based factors combine to give an average contribution of 21% over the entire year. The monthly contributions

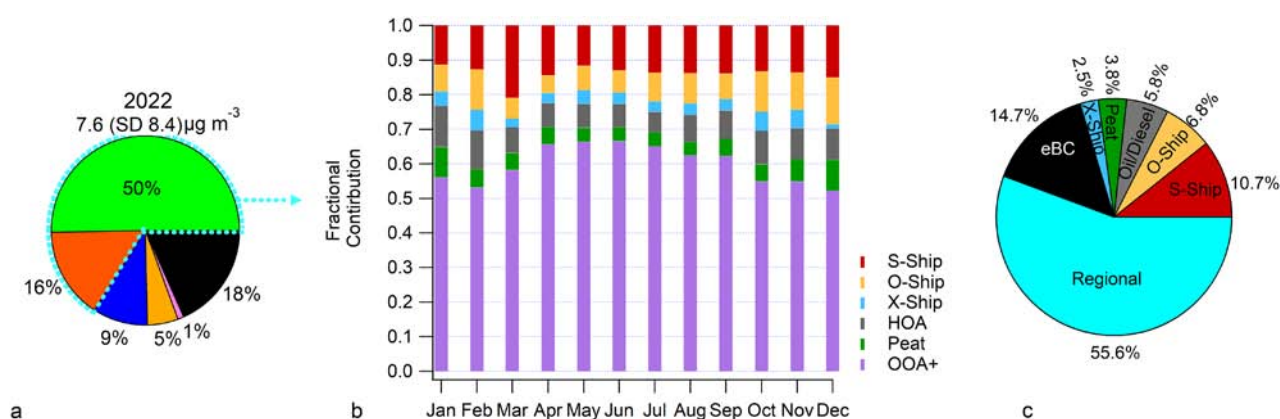


Figure 3.17. (a) Pie chart of Q-ACSM species and eBC for 2022. (b) Bar chart of the monthly contribution of PMF resolved factors, including S-Ship, O-Ship, X-Ship, HOA, peat and OOA+ (OOA and regional sulfate), in 2022. The blue dashed highlighted area in (a) shows OA–SO₄²⁻ input that is resolved by the PMF in (b). (c) Pie chart showing source contribution estimates to PM_{2.5} with adjusted O-Ship, S-Ship and eBC, as in Figure 3.11b.

(Figure 3.17b) show a degree of variation, with winter months having more primary combustion sources (e.g. peat) and summer having more regional OA contribution. However, regional contributions were also high in March and April, but this was due to higher inorganic loading, primarily NO_3^- , and not just due to regional OA.

Interestingly, the diurnal pattern of both S-Ship and O-Ship remain consistent over the seasons (Figures 3.18 and 3.19), while the monthly concentrations tend to have a maximum in winter months, coinciding with the increased shipping activity prior to Christmas. This may be less clear in the S-Ship monthly trends (Figure 3.17a), as the S-Ship factor is still somewhat affected by regional SO_4^{2-} and therefore influenced to a degree by the seasonal cycle of non-ship-related SO_4^{2-} .

3.6 Impact of Port Emissions on Dublin Air Quality

The measurements and analysis presented so far are specifically related to the selected measurement site in Dublin Port and cannot be used to directly assess the impact of port emissions on Dublin air quality.

Moreover, the port is located east of Dublin city centre, which means that the prevailing westerly winds will carry emissions from ships and other port-related activities towards the Irish Sea. However, air pollution from the port can be carried over the city under different wind directions. To assess the impact of port emissions on air quality, meteorological analysis was combined with (i) the measurements made by the air sensor network positioned around the periphery of the port area, and (ii) SO_2 measurements made at various stations in the national air quality monitoring network. Details of these two approaches are outlined below.

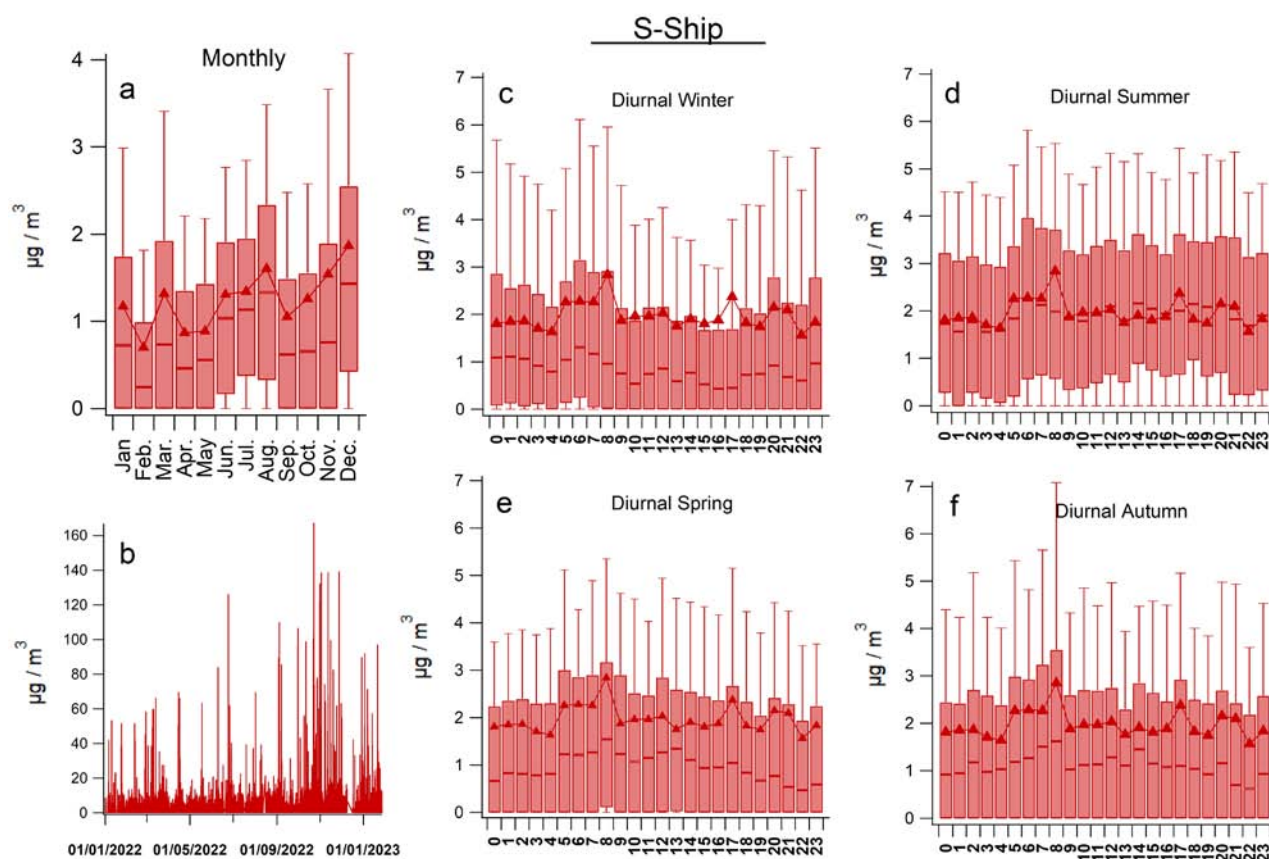


Figure 3.18. S-Ship factor overview of (a) monthly concentrations; (b) the time series; (c) diurnal (concentration vs hour of the day) winter concentrations; (d) diurnal summer concentrations; (e) diurnal spring concentrations; and (f) diurnal autumn concentrations. In panels (a) and (c)–(f), the triangle markers and error bars show mean and standard deviation, while the box plots show medians and percentiles.

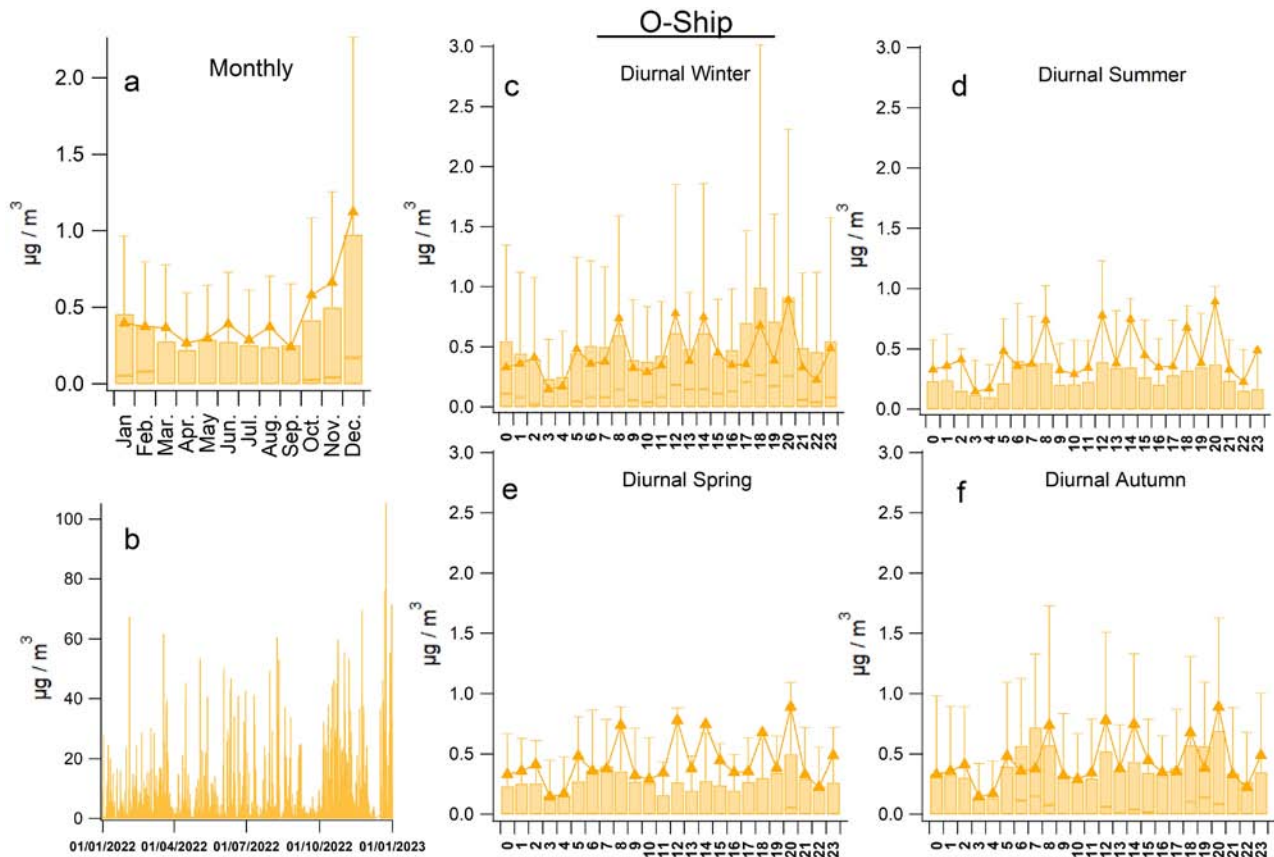


Figure 3.19. O-Ship factor overview of (a) monthly concentrations; (b) the time series; (c) diurnal (concentration vs hour of the day) winter concentrations; (d) diurnal summer concentrations; (e) diurnal spring concentrations; and (f) diurnal autumn concentrations. In panels (a) and (c)–(f), the triangle markers and error bars show mean and standard deviation, while the box plots show medians and percentiles.

3.6.1 Estimates based on $PM_{2.5}$ measurements

Data generated by air sensors deployed at Promenade Road, North Wall Quay and Ringsend were selected as being the most relevant for assessing the transport of port emissions to the city centre. The relationship between wind direction/speed and $PM_{2.5}$ concentration at each of these locations, as well as the main PortAIR site, is represented in the polar plots shown in Figure 3.20. The plots appear to be very similar but do contain small statistical differences, which are revealed in the analysis.

The approach involves separating the $PM_{2.5}$ measured by each sensor into two different wind sectors – “Port” and “City”. The split between “Port” and “City” wind sectors for the sensors at Promenade Road and North Wall Quay is the north–south line, with “Port” being defined as the air moving from east to west (wind sector 0 to 180 degrees). For Ringsend, “Port” is

defined as air moving from the north-east in the sector 340 to 110 degrees. The results show that the average $PM_{2.5}$ concentrations measured at the three locations were higher when experiencing air transported from the “Port” rather than from the “City” (Table 3.6). In other words, at these locations, air coming from the port was more polluted than air coming from the city. Moreover, one-way analysis of variance suggests that the difference in average $PM_{2.5}$ levels between the two wind sectors was statistically significant ($p < 0.05$) and was thus highly unlikely to be caused by random variation.

The overall impact of the “Port” sector on the $PM_{2.5}$ levels in each location can be estimated from its impact on the overall average $PM_{2.5}$ levels for the full measurement period. Assuming that the $PM_{2.5}$ levels measured during city-influenced air masses are independent of the port sector, then it logically follows

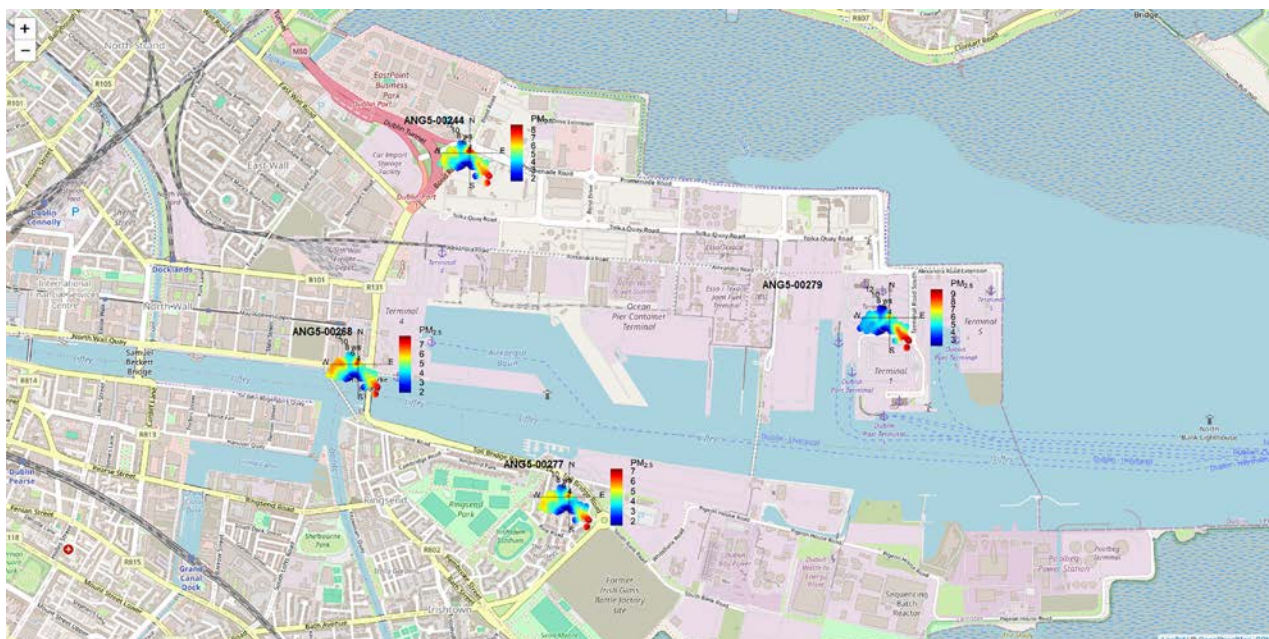


Figure 3.20. Polar plots to show the relationship between wind direction/speed and $PM_{2.5}$ concentration at four locations in the air sensor network around Dublin Port: Promenade Road (ANG5-00244), North Wall Quay (ANG5-00268), Ringsend (ANG5-00277) and PortAIR (ANG5-00279). Wind data are taken from the PortAIR sampling site, with data omitted at wind speeds < 2 m/s.

Table 3.6. Comparison of $PM_{2.5}$ concentrations ($\mu g m^{-3}$) measured during “Port” and “City” influenced air masses

| Location | Overall average $PM_{2.5}$ | “Port” average $PM_{2.5}$ | “City” average $PM_{2.5}$ | p -value | % of hours from “City” sector | % of hours from “Port” sector | Extra $PM_{2.5}$ from “Port” |
|-----------------|----------------------------|---------------------------|---------------------------|------------------------|-------------------------------|-------------------------------|------------------------------|
| Promenade Road | 5.60 | 6.06 | 5.31 | 3.27×10^{-8} | 62.0 | 38.0 | 5.40 |
| North Wall Quay | 5.03 | 5.56 | 4.74 | 2.52×10^{-11} | 65.3 | 34.7 | 5.90 |
| Ringsend | 4.41 | 5.24 | 4.28 | 1.92×10^{-2} | 87.2 | 12.8 | 2.90 |

that the difference between the “City” $PM_{2.5}$ and the overall average $PM_{2.5}$ for the full measurement period must be due to the influence of the “Port” wind sector. Therefore, an approximation of the influence of the “Port” sector can be given by:

additional $PM_{2.5}$ load from “Port” sector over and beyond “City” average = (overall average $PM_{2.5}$ – “City” average $PM_{2.5}$) / (“City” average $PM_{2.5}$).

The results, shown in Table 3.6, indicate that when the wind comes from the direction of the port, the average $PM_{2.5}$ concentration is increased by 5–6% in locations at the western boundary of Dublin Port (Promenade Road and North Wall Quay), and by around 3% in Ringsend.

3.6.2 Estimates based on SO_2 measurements

Meteorological analysis was also combined with SO_2 measurements to estimate the impact of shipping emissions on Dublin city. Although SO_2 was not measured by the sensors deployed in the PortAIR project, it was measured using reference instruments at two nearby monitoring sites in the national air quality monitoring network: Ringsend (Station 17) and Winetavern Street (Station 11). The analysis approach for SO_2 was the same as that for $PM_{2.5}$, but instead used daily average wind directions from Dublin Airport provided by Met Éireann, which were deemed to be more representative of the synoptic wind patterns influencing the city centre. The wind sector for “Port” influence at Ringsend is as defined above. Winetavern

Street is further from the port and its influence cannot be isolated based on wind direction alone, thus the “Port” sector here is simply defined as easterly winds, in the sector 0 to 180 degrees.

For Winetavern Street, the average SO_2 concentrations were $1.38 \mu\text{g m}^{-3}$ for the “Port” sector and $1.47 \mu\text{g m}^{-3}$ for the “City” sector, but the difference was not statistically significant ($p > 0.05$). For Ringsend, the sectoral averages were statistically significant, with $3.67 \mu\text{g m}^{-3}$ for the “Port” sector and $2.7 \mu\text{g m}^{-3}$ for the “City” sector, compared with an overall average of $2.88 \mu\text{g m}^{-3}$. Thus, the average SO_2 concentration experienced at Ringsend was 6.4%

higher due to the influence of wind masses coming from the “Port” sector.

This simple analysis of measurements performed under the meteorological conditions encountered in 2022 suggests that parts of the city directly adjacent to the port experience slightly elevated levels of air pollution due to emissions coming from the port. Further measurements and analysis, possibly involving modelling approaches, are required to deliver more robust estimates of the impact of port-based emissions on Dublin air quality, especially to evaluate the impact of port emissions on the city during stagnant weather conditions.

4 Conclusions and Recommendations

4.1 Conclusions

An extensive range of state-of-the-art instrumentation for real-time measurements of $PM_{2.5}$ chemical composition and pollutant gases was successfully deployed at a monitoring location in Dublin Port for a period of 14 months (December 2021 to February 2023). The data have been used to develop source apportionment models for quantifying the contribution of ship emissions and other sources to ambient levels of air pollution in the Dublin Port area.

The annual mean concentrations of both NO_2 and SO_2 at the PortAIR site were within the current EU CAFE Directive limits and also within the revised annual limit values to be attained by 1 January 2030. However, the NO_2 mean concentration did exceed the WHO AQG value of $10 \mu g m^{-3}$. Both pollutants exhibited numerous intense spikes throughout the year due to local combustion sources, including road vehicles and ships. High levels of NO_x ($NO + NO_2$) were also measured at the PortAIR site, and, while the EU annual critical load value of $30 \mu g m^{-3}$ is not directly applicable to urban monitoring locations, the NO_x emissions could impact on the Bull Island Special Protection Area, which is situated only a few kilometres downwind of the port.

The annual mean concentration of $PM_{2.5}$ at the PortAIR site for the calendar year 2022 ($7.6 \mu g m^{-3}$) was within the current EU CAFE Directive limits and also within the revised annual limit value to be attained by 1 January 2030. However, it did exceed the WHO AQG annual mean value of $5 \mu g m^{-3}$, and, in addition, the 24-hour AQG value of $15 \mu g m^{-3}$ was surpassed on 25 days in 2022. Results from a network of nine air sensors deployed around the port showed that mean $PM_{2.5}$ levels around the port were similar, but exhibited different spikes in pollution due to variations in emissions from traffic and other hyperlocal sources. Data from the sensor network were combined with meteorological analysis to show that, in 2022, emissions carried from the port wind sector caused an estimated average increase of up to 6% in $PM_{2.5}$ in parts of the city directly adjacent to the port.

The online measurements of chemical composition showed that, on average, in 2022, the $PM_{2.5}$ measured at the PortAIR site was composed of 50% OA, 19% eBC, 16% SO_4^{2-} , 9% NO_3^- , 5% NH_4^+ and 1% Cl^- . Complementary offline chemical analysis indicated the presence of carbon, Na, magnesium, sulfur and chlorine as the most abundant elemental species in $PM_{2.5}$.

The Q-ASCM and Xact instruments were combined during the intensive measurement period to identify ship plumes and subsequently provide a more detailed analysis of their chemical composition. The plumes were observed as discrete pollution events, with known markers including V and Ni, SO_2 and NO_x , eBC and OA, with a mass spectral profile indicative of fossil fuel burning. PMF of the organic and SO_4^{2-} components measured by the Q-ACSM identified two main types of ship emissions – one type dominated by SO_4^{2-} (S-Ship) and the other type dominated by OA (O-Ship). Close investigation of these source factors, information on vessel fuel use, wind direction and shipping logs indicated that S-Ship particles originated from ships using high-sulfur HFO with a scrubber system, and O-Ship particles were emitted by ships that use low-sulfur marine fuels, primarily VLSFO. These two distinct types of ship emission profiles enable organic- SO_4^{2-} source apportionment with the advantage of distinguishing scrubbed HFO emissions from VLSFO fuel emissions without the use of tracers. A third minor ship emission factor (X-Ship) was resolved by PMF but not clearly attributable to any specific fuel type. Supplementary source apportionment of the Xact data indicated the presence of other sources of $PM_{2.5}$, which may include sea salt, resuspended crustal material and non-exhaust emissions from vehicles.

Ship plumes were observed to last up to 2.5 hours given steady wind direction and fuel use while a ship was in port. However, the more extreme pollution peaks ($PM_{10} > 53.5 \mu g m^{-3}$) lasted only 5–35 minutes and were caused specifically when ships were manoeuvring in and out of berth. While hoteling periods at dock were characterised by lower PM mass concentrations, the particle number concentrations

remained extremely high for submicron particles ($d_m < 50$ nm), especially when ships were switched over to MGO for power. In fact, MGO emissions were characterised only by these large number concentrations of small particles, as PM mass concentrations were neither clearly noticeable as plumes ($PM_{10} < 15 \mu g m^{-3}$) nor from the mass spectra of OA, mostly due to instrumental limitations of measuring these very small particles with an ACSM. This limitation leads to an underestimation of the contribution of low-sulfur fuels to PM_{10} and highlights the need for monitoring the aerosol number–size distribution in ship emission studies.

Source apportionment modelling to quantify source contributions to $PM_{2.5}$ was subsequently conducted for the period 1 January to 31 December 2022, based on the continuously collected Q-ACSM data. Overall, the $PM_{2.5}$ breakdown for 2022 was 56% regional contribution, 15% eBC, 11% S-Ship, 7% O-Ship, 6% HOA, 4% peat and 3% X-Ship. The ship-based factors thus combined to give an average contribution of 21% to $PM_{2.5}$ at the PortAIR site. While the diurnal pattern of both S-Ship and O-Ship remained consistent across the year, the monthly concentrations showed some variation and exhibited a maximum in winter months, coinciding with the increased shipping activity prior to Christmas. The peat contribution was also higher during winter, whereas summer had more regional OA contribution.

Despite the short-lived nature of ship plumes in Dublin Port, S-Ship and O-Ship combine to contribute a significant fraction of $PM_{2.5}$ and submicron particle number concentration in the port area, with the potential to increase even further with the planned port activity expansion. With more and more ships investing in low-sulfur and alternative fuels, future studies on air quality in ports will be needed to better capture and investigate the very high concentrations of small particles (<50 nm diameter) expected from “cleaner” fuels, including MGO, as there are potentially serious implications for particle transport, toxicity and climate forcing.

4.2 Recommendations

The PortAIR project has produced a wealth of new information on the sources of air pollution in Dublin Port. Primary shipping emissions contributed at least 21% to $PM_{2.5}$ and were a major source of NO_x during

both manoeuvring and hoteling periods. The following recommendations are made in relation to reducing emissions that impact on air quality and health.

- Measures should be taken to reduce NO_x emissions from ships and road vehicles in the port area. These measures could be incorporated into an air quality action plan specifically for Dublin Port and also feature in the overall plan for air quality management in the Dublin city area. The most obvious measure to reduce NO_x emissions from ships is to provide shore-side electricity to ships at berth, which is included in the Alternative Fuels Infrastructure Regulations and is also referenced in the Dublin Port Masterplan 2040. This could lead to “zero on-site emissions” of all pollutants during the hoteling phase, and although emissions from power stations adjacent to the port may be elevated as a result, these emissions are more closely monitored and regulated than those from ships.
- Another potential measure to reduce pollution from ships is for Dublin Port to be part of a designated Emission Control Area (ECA) for NO_x . This would require ships to install abatement technology, such as selective catalytic reduction, which would significantly reduce the large amounts of NO_x emitted during manoeuvring. Indeed, since 2022, Ireland has worked with the UK, Portugal, France, Spain, Greenland, Iceland and the Faroe Islands on a proposal to designate an ECA in the North-East Atlantic. If introduced, the ECA would not only control NO_x emissions from ships around Ireland, but also reduce sulfur oxides and PM.
- The use of battery-powered ferries and small vessels is increasing worldwide and their introduction in Dublin Port would reduce emissions of air pollutants and CO_2 .
- Government departments and agencies should investigate the pros and cons associated with switching to renewable and low-carbon fuels for ships. While these fuels may be expected to produce low or even zero greenhouse gas emissions, research needs to be undertaken to also assess potential impacts of alternative fuels on air quality and health.

This research clearly demonstrated the value of the SMPS and Xact instruments for online continuous monitoring of particle number concentrations and

elements, respectively. Further evidence was obtained to support the use of calibrated sensor networks to assess the variation in $PM_{2.5}$ across areas with a range of activities and emission sources. The following recommendations are made in relation to conducting research on the chemical composition and sources of particles that impact on air quality and health.

- Instruments such as the SMPS are essential for monitoring particle number concentration and size distribution, and should be utilised in a wider range of research projects on atmospheric particles. Moreover, the inclusion of particle number concentration and particle size distribution as metrics in the new EU Ambient Air Quality Directive also necessitates the deployment of instruments such as SMPS in ongoing national air quality monitoring programmes (EU, 2008). It is therefore recommended that investment is made in this area of research and monitoring to provide a detailed assessment of the presence and sources of ultrafine particles, which are especially harmful due to their ability to penetrate deep into

the respiratory, cardiovascular and blood–brain barrier systems.

- Further efforts should be made to deploy $PM_{2.5}$ sensor networks in urban locations, including in areas such as ports where there are many local pollution sources. When calibrated against reference instruments, the sensors can provide good-quality data to assess the spatial variation of air pollution and provide insights into sources. It is recommended that studies are also conducted to assess the potential for sensors to be incorporated into air monitoring strategies and how they can best complement the data obtained by the national network.
- Online elemental analysis of PM using instruments such as the Xact is extremely useful for identifying pollution sources that are not detected by the ACSM. It is therefore recommended that future highly instrumented field measurement campaigns utilise online elemental analysis to provide a more complete understanding of both the anthropogenic and natural sources of PM.

References

- ACTRIS (Aerosol, Clouds and Trace Gases Research Infrastructure), 2021. CAIS-ECAC – Center for Aerosol In-Situ – European Center for Aerosol Calibration and Characterization. Available online: <https://www.actris-ecac.eu/pmc-non-refractory-organics-and-inorganics.html> (accessed 25 June 2025).
- Agrawal, H., Eden, R., Zhang, X., Fine, P. M., Katzenstein, A., Miller, J. W., Ospital, J., Teffera, S. and Cocker, D. R., III, 2009. Primary particulate matter from ocean-going engines in the southern California air basin. *Environmental Science & Technology* 43: 5398–5402. <https://doi.org/10.1021/es8035016>
- Anders, L., Schade, J., Rosewig, E. I., Kroeger-Badge, T., Irsig, R., Jeong, S., Bendl, J., Saraji-Bozorgzad, M., Huang, J.-H., Zhang, F.-Y., Wang, C. C., Adam, T., Sklorz, M., Etzien, U., Buchholz, B., Czech, H., Streibel, T., Passig, J. and Zimmermann, R., 2023. Detection of ship emissions from distillate fuel operation via single-particle profiling of polycyclic aromatic hydrocarbons. *Environmental Science: Atmospheres* 3: 1134–1144. <https://doi.org/10.1039/D3EA00056G>
- Bond, T. C., Doherty, S. J., Fahey, D. W., Forster, P. M., Berntsen, T., DeAngelo, B. J., Flanner, M. G., Ghan, S., Kärcher, B., Koch, D., Kinne, S., Kondo, Y., Quinn, P. K., Sarofim, M. C., Schultz, M. G., Schulz, M., Venkataraman, C., Zhang, H., Zhang, S., Bellouin, N., Guttikunda, S. K., Hopke, P. K., Jacobson, M. Z., Kaiser, J. W., Klimont, Z., Lohmann, U., Schwarz, J. P., Shindell, D., Storelvmo, T., Warren, S. G. and Zender, C. S., 2013. Bounding the role of black carbon in the climate system: a scientific assessment. *JGR Atmospheres* 118: 5380–5552. <https://doi.org/10.1002/jgrd.50171>
- Canonaco, F., Crippa, M., Slowik, J. G., Baltensperger, U. and Prévôt, A. S. H., 2013. SoFi, an IGOR-based interface for the efficient use of the generalized multilinear engine (ME-2) for the source apportionment: ME-2 application to aerosol mass spectrometer data. *Atmospheric Measurement Techniques* 6: 3649–3661. <https://doi.org/10.5194/amt-6-3649-2013>
- Chazeau, B., El Haddad, I., Canonaco, F., Temime-Roussel, B., D’Anna, B., Gille, G., Mesbah, B., Prévôt, A. S. H., Wortham, H. and Marchand, N., 2022. Organic aerosol source apportionment by using rolling positive matrix factorization: application to a Mediterranean coastal city. *Atmospheric Environment: X* 14: 100176. <https://doi.org/10.1016/j.aeaoa.2022.100176>
- Collins, D. R., Cocker, D. R., Flagan, R. C. and Seinfeld, J. H., 2004. The scanning DMA transfer function. *Aerosol Science and Technology* 38: 833–850. <https://doi.org/10.1080/027868290503082>
- CSO (Central Statistics Office), 2019. Transport Omnibus 2019. Available online: <https://www.cso.ie/en/releasesandpublications/ep/p-tranom/transportomnibus2019/> (accessed 20 June 2025).
- Czech, H., Schnelle-Kreis, J., Streibel, T. and Zimmermann, R., 2017. New directions: beyond sulphur, vanadium and nickel – about source apportionment of ship emissions in emission control areas. *Atmospheric Environment* 163: 190–191. <https://doi.org/10.1016/j.atmosenv.2017.05.017>
- Davison, A. C. and Hinkley, D. V., 1997. *Bootstrap Methods and their Application*, Cambridge Series in Statistical and Probabilistic Mathematics. Cambridge University Press, Cambridge. <https://doi.org/10.1017/CBO9780511802843>
- DPC (Dublin Port Company), 2018. Masterplan 2040. Available online: <https://www.dublinport.ie/masterplan/masterplan-2040-reviewed-2018/> (accessed 25 June 2025).
- Drinovec, L., Močnik, G., Zotter, P., Prévôt, A. S. H., Ruckstuhl, C., Coz, E., Rupakheti, M., Sciare, J., Müller, T., Wiedensohler, A. and Hansen, A. D. A., 2015. The “dual-spot” Aethalometer: an improved measurement of aerosol black carbon with real-time loading compensation. *Atmospheric Measurement Techniques* 8: 1965–1979. <https://doi.org/10.5194/amt-8-1965-2015>
- EEA (European Environment Agency), 2013. The impact of international shipping on European air quality and climate forcing, 4/2013. Available online: <https://www.eea.europa.eu/en/analysis/publications/the-impact-of-international-shipping> (accessed 25 June 2025).
- EEA (European Environment Agency), 2025a. Greenhouse gas emissions from transport in Europe. Available online: <https://www.eea.europa.eu/en/analysis/indicators/greenhouse-gas-emissions-from-transport/greenhouse-gas-emissions-from-transport> (accessed 25 June 2025).
- EEA (European Environment Agency), 2025b. *European Maritime Transport Environmental Report 2025*. Available online: <https://www.eea.europa.eu/en/analysis/publications/maritime-transport-2025> (accessed 25 June 2025).

- Efron, B., 1979. Bootstrap methods: another look at the jackknife. *The Annals of Statistics* 7: 1–26. <https://doi.org/10.1214/aos/1176344552>
- Eichler, P., Müller, M., Rohmann, C., Stengel, B., Orasche, J., Zimmermann, R. and Wisthaler, A., 2017. Lubricating oil as a major constituent of ship exhaust particles. *Environmental Science and Technology Letters* 4: 54–58. <https://doi.org/10.1021/acs.estlett.6b00488>
- EPA (Environmental Protection Agency), 2025. AirQuality.ie. Available online: <https://airquality.ie/> (accessed 25 June 2025).
- EU (European Union), 2008. Directive 2008/50/EC of the European Parliament and of the Council of 21 May 2008 on ambient air quality and cleaner air for Europe. OJ L 152, 11.6.2008, pp. 1–44.
- Fossum, K. N., Lin, C., O'Sullivan, N., Lei, L., Hellebust, S., Ceburnis, D., Afzal, A., Tremper, A., Green, D., Jain, S., Byčenkienė, S., O'Dowd, C., Wenger, J. and O'vadnevaite, J., 2024. Two distinct ship emission profiles for organic-sulfate source apportionment of PM in sulfur emission control areas. *Atmospheric Chemistry and Physics* 24: 10815–10831. <https://doi.org/10.5194/acp-24-10815-2024>
- Furger, M., Minguillón, M. C., Yadav, V., Slowik, J. G., Hüglin, C., Fröhlich, R., Petterson, K., Baltensperger, U. and Prévôt, A. S. H., 2017. Elemental composition of ambient aerosols measured with high temporal resolution using an online XRF spectrometer. *Atmospheric Measurement Techniques* 10: 2061–2076. <https://doi.org/10.5194/amt-10-2061-2017>
- Healy, R. M., O'Connor, I. P., Hellebust, S., Allanic, A., Sodeau, J. R. and Wenger, J. C., 2009. Characterisation of single particles from in-port ship emissions. *Atmospheric Environment* 43: 6408–6414. <https://doi.org/10.1016/j.atmosenv.2009.07.039>
- Healy, R. M., Hellebust, S., Kourtchev, I., Allanic, A., O'Connor, I. P., Bell, J. M., Healy, D. A., Sodeau, J. R. and Wenger, J. C., 2010. Source apportionment of PM_{2.5} in Cork Harbour, Ireland using a combination of single particle mass spectrometry and quantitative semi-continuous measurements. *Atmospheric Chemistry and Physics* 10: 9593–9613. <https://doi.org/10.5194/acp-10-9593-2010>
- Hong, W.-J., Dong, W.-J., Zhao, T.-T., Zheng, J.-Z., Lu, Z.-G. and Ye, C., 2023. Ambient PM_{2.5}-bound polycyclic aromatic hydrocarbons in Ningbo Harbor, eastern China: seasonal variation, source apportionment, and cancer risk assessment. *Air Quality, Atmosphere & Health* 16: 1809–1821. <https://doi.org/10.1007/s11869-023-01373-6>
- Lin, C., Huang, R.-J., Ceburnis, D., Buckley, P., Preissler, J., Wenger, J., Rinaldi, M., Facchini, M. C., O'Dowd, C. and O'vadnevaite, J., 2018. Extreme air pollution from residential solid fuel burning. *Nature Sustainability* 1: 512–517. <https://doi.org/10.1038/s41893-018-0125-x>
- Lin, C., Ceburnis, D., Huang, R. J., Xu, W., Spohn, T., Martin, D., Buckley, P., Wenger, J., Hellebust, S., Rinaldi, M., Facchini, M. C., O'Dowd, C. and O'vadnevaite, J., 2019. Wintertime aerosol dominated by solid-fuel-burning emissions across Ireland: insight into the spatial and chemical variation in submicron aerosol. *Atmospheric Chemistry and Physics* 19: 14091–14106. <https://doi.org/10.5194/acp-19-14091-2019>
- Lin, C., Ceburnis, D., Xu, W., Heffernan, E., Hellebust, S., Gallagher, J., Huang, R. J., O'Dowd, C. and O'vadnevaite, J., 2020. The impact of traffic on air quality in Ireland: insights from the simultaneous kerbside and suburban monitoring of submicron aerosols. *Atmospheric Chemistry and Physics* 20: 10513–10529. <https://doi.org/10.5194/acp-20-10513-2020>
- Lin, C., Ceburnis, D., Trubetskaya, A., Xu, W., Smith, W., Hellebust, S., Wenger, J., O'Dowd, C. and O'vadnevaite, J., 2021. On the use of reference mass spectra for reducing uncertainty in source apportionment of solid-fuel burning in ambient organic aerosol. *Atmospheric Measurement Techniques* 14: 6905–6916. <https://doi.org/10.5194/amt-14-6905-2021>
- MARPOL Training Institute, 2006. Annex VI – Regulations for the Prevention of Air Pollution from Ships. Available online: https://www.marpoltraininginstitute.com/MMSKOREAN/MARPOL/Annex_VI/index.htm (accessed 25 June 2025).
- Mazzei, F., D'Alessandro, A., Lucarelli, F., Nava, S., Prati, P., Valli, G., and Vecchi, R., 2008. Characterization of particulate matter sources in an urban environment. *Science of The Total Environment* 401: 81–89. <https://doi.org/10.1016/j.scitotenv.2008.03.008>
- Mueller, D., Uibel, S., Takemura, M., Klingelhofer, D. and Groneberg, D. A., 2011. Ships, ports and particulate air pollution – an analysis of recent studies. *Journal of Occupational Medicine and Toxicology* 6: 31. <https://doi.org/10.1186/1745-6673-6-31>
- Mueller, N., Westerby, M. and Nieuwenhuijsen, M., 2023. Health impact assessments of shipping and port-sourced air pollution on a global scale: a scoping literature review. *Environmental Research* 216(1): 114460.

- Ng, N. L., Herndon, S. C., Trimborn, A., Canagaratna, M. R., Croteau, P. L., Onasch, T. B., Sueper, D., Worsnop, D. R., Zhang, Q., Sun, Y. L. and Jayne, J. T., 2011. An aerosol chemical speciation monitor (ACSM) for routine monitoring of the composition and mass concentrations of ambient aerosol. *Aerosol Science and Technology* 45: 780–794. <https://doi.org/10.1080/02786826.2011.560211>
- O'Connor, I. P., Allanic, A., Hellebust, S., Kourtchev, I., Healy, R. M., Healy, D. A., Bell, J. M., Wenger, J. C. and Sodeau, J. R., 2013. *Composition and Sources of Particulate Air Pollution in a Port Environment, Cork, Ireland*. Environmental Protection Agency, Johnstown Castle, Ireland.
- Ovadnevaite, J., Lin, C., Rinaldi, M., Ceburnis, D., Buckley, P., Coleman, L., Facchini, M. C., Wenger, J. and O'Dowd, C., 2021. *Air Pollution Sources in Ireland*. Environmental Protection Agency, Johnstown Castle, Ireland.
- Paatero, P., 1997. Least squares formulation of robust non-negative factor analysis. *Chemometrics and Intelligent Laboratory Systems* 37: 23–35. [https://doi.org/10.1016/S0169-7439\(96\)00044-5](https://doi.org/10.1016/S0169-7439(96)00044-5)
- Paatero, P., 1999. The multilinear engine: a table-driven, least squares program for solving multilinear problems, including the n-way parallel factor analysis model. *Journal of Computational and Graphical Statistics* 8: 854888. <https://doi.org/10.2307/1390831>
- Paatero, P., Eberly, S., Brown, S. G. and Norris, G. A., 2014. Methods for estimating uncertainty in factor analytic solutions. *Atmospheric Measurement Techniques* 7: 781–797. <https://doi.org/10.5194/amt-7-781-2014>
- Pandolfi, M., Gonzalez-Castanedo, Y., Alastuey, A., de la Rosa, J. D., Mantilla, E., de la Campa, A. S., Querol, X., Pey, J., Amato, F. and Moreno, T., 2011. Source apportionment of PM₁₀ and PM_{2.5} at multiple sites in the strait of Gibraltar by PMF: impact of shipping emissions. *Environmental Science and Pollution Research* 18: 260–269. <https://doi.org/10.1007/s11356-010-0373-4>
- Petzold, A., Ogren, J. A., Fiebig, M., Laj, P., Li, S. M., Baltensperger, U., Holzer-Popp, T., Kinne, S., Pappalardo, G., Sugimoto, N., Wehrli, C., Wiedensohler, A. and Zhang, X. Y., 2013. Recommendations for reporting “black carbon” measurements. *Atmospheric Chemistry and Physics* 13: 8365–8379. <https://doi.org/10.5194/acp-13-8365-2013>
- Tong, M., Zhang, Y., Zhang, H., Chen, D., Pei, C., Guo, H., Song, W., Yang, X. and Wang, X., 2024. Contribution of ship emission to volatile organic compounds based on one-year monitoring at a coastal site in the Pearl River Delta region. *Journal of Geophysical Research: Atmospheres* 129: e2023JD039999. <https://doi.org/10.1029/2023JD039999>
- Tremper, A. H., Font, A., Priestman, M., Hamad, S. H., Chung, T. C., Pribadi, A., Brown, R. J. C., Goddard, S. L., Grassineau, N., Petterson, K., Kelly, F. J. and Green, D. C., 2018. Field and laboratory evaluation of a high time resolution X-ray fluorescence instrument for determining the elemental composition of ambient aerosols. *Atmospheric Measurement Techniques* 11: 3541–3557. <https://doi.org/10.5194/amt-11-3541-2018>
- Ulbrich, I. M., Canagaratna, M. R., Zhang, Q., Worsnop, D. R. and Jimenez, J. L., 2009. Interpretation of organic components from Positive Matrix Factorization of aerosol mass spectrometric data. *Atmospheric Chemistry and Physics* 9: 2891–2918. <https://doi.org/10.5194/acp-9-2891-2009>
- Viana, M., Amato, F., Alastuey, A., Querol, X., Moreno, T., García Dos Santos, S., Herce, M. D. and Fernández-Patier, R., 2009. Chemical tracers of particulate emissions from commercial shipping. *Environmental Science & Technology* 43: 7472–7477. <https://doi.org/10.1021/es901558t>
- Yang, J., Tang, T., Jiang, Y., Karavalakis, G., Durbin, T. D., Wayne Miller, J., Cocker, D. R. and Johnson, K. C., 2021. Controlling emissions from an ocean-going container vessel with a wet scrubber system. *Fuel* 304: 121323. <https://doi.org/10.1016/j.fuel.2021.121323>
- Yau, P. S., Lee, S. C., Cheng, Y., Huang, Y., Lai, S. C. and Xu, X. H., 2013. Contribution of ship emissions to the fine particulate in the community near an international port in Hong Kong. *Atmospheric Research* 124: 61–72. <https://doi.org/10.1016/j.atmosres.2012.12.009>
- Zetterdahl, M., Moldanová, J., Pei, X., Pathak, R. K. and Demirdjian, B., 2016. Impact of the 0.1% fuel sulfur content limit in SECA on particle and gaseous emissions from marine vessels. *Atmospheric Environment* 145: 338–345. <https://doi.org/10.1016/j.atmosenv.2016.09.022>
- Zhao, M., Zhang, Y., Ma, W., Fu, Q., Yang, X., Li, C., Zhou, B., Yu, Q. and Chen, L., 2013. Characteristics and ship traffic source identification of air pollutants in China's largest port. *Atmospheric Environment* 64: 277–286. <https://doi.org/10.1016/j.atmosenv.2012.10.007>

Abbreviations

| | |
|-------------------------|---|
| ACSM | Aerosol chemical speciation monitor |
| AQG | Air quality guideline |
| BDL | Below detection limit |
| CAFE | Clean Air For Europe |
| eBC | Equivalent black carbon |
| EC | Elemental carbon |
| ECA | Emission Control Area |
| EU | European Union |
| EUSAAR2 | European Supersites for Atmospheric Aerosol Research |
| HFO | Heavy fuel oil |
| HOA | Hydrocarbon-like organic aerosol |
| LPM | Litres per minute |
| ME-2 | Multilinear Engine version 2 |
| MGO | Marine gas oil |
| m/m | Mass by mass |
| OA | Organic aerosol |
| OC | Organic carbon |
| OOA | Oxygenated organic aerosol |
| O-Ship | Organic-rich ship emissions |
| PM | Particulate matter |
| PM₁ | Particulate matter with a diameter of less than 1 micron |
| PM_{2.5} | Particulate matter with a diameter of less than 2.5 microns |
| PM₁₀ | Particulate matter with a diameter of less than 10 microns |
| PMF | Positive matrix factorisation |
| ppb | Parts per billion |
| ppm | Parts per million |
| Q-ACSM | Quadrupole aerosol chemical speciation monitor |
| SMPS | Scanning mobility particle sizer |
| S-Ship | Sulfate-rich ship emissions |
| UCD | University College Dublin |
| ULSFO | Ultra-low-sulfur fuel oil |
| VLSFO | Very-low-sulfur fuel oil |
| WHO | World Health Organization |
| Xact | Xact Ambient Continuous Multi-Metals Monitor |
| XRF | X-ray fluorescence |

An Ghníomhaireacht Um Chaomhnú Comhshaoil

Tá an GCC freagrach as an gcomhshaol a chosaint agus a fheabhsú, mar shócmhainn luachmhar do mhuintir na hÉireann. Táimid tiomanta do dhaoine agus don chomhshaol a chosaint ar thionchar díobhálach na radaíochta agus an truaillithe.

Is féidir obair na Gníomhaireachta a roinnt ina trí phríomhréimse:

Rialáil: Rialáil agus córais chomhlíonta comhshaoil éifeachtacha a chur i bhfeidhm, chun dea-thorthaí comhshaoil a bhaint amach agus díriú orthu siúd nach mbíonn ag cloí leo.

Eolas: Sonraí, eolas agus measúnú ardchaighdeán, spriocdhírthe agus tráthúil a chur ar fáil i leith an chomhshaoil chun bonn eolais a chur faoin gcinnteoireacht.

Abhcóideacht: Ag obair le daoine eile ar son timpeallachta glaine, táirgiúla agus dea-chosanta agus ar son cleachtas inbhuanaithe i dtaobh an chomhshaoil.

I measc ár gcuid freagrachtaí tá:

Ceadúnú

- > Gníomhaíochtaí tionscail, dramhaíola agus stórála peitрил ar scála mór;
- > Sceitheadh fuíolluisce uirbigh;
- > Úsáid shrianta agus scaoileadh rialaithe Orgánach Géinmhodhnaithe;
- > Foinsí radaíochta ianúcháin;
- > Astaíochtaí gás ceaptha teasa ó thionscal agus ón eitlíocht trí Scéim an AE um Thrádáil Astaíochtaí.

Forfheidhmiú Náisiúnta i leith Cúrsaí Comhshaoil

- > Iniúchadh agus cigireacht ar shaoráidí a bhfuil ceadúnas acu ón GCC;
- > Cur i bhfeidhm an dea-chleachtais a stiúradh i ngníomhaíochtaí agus i saoráidí rialáilte;
- > Maoirseacht a dhéanamh ar fhreagrachtaí an údaráis áitiúil as cosaint an chomhshaoil;
- > Caighdeán an uisce óil phoiblí a rialáil agus údaruithe um sceitheadh fuíolluisce uirbigh a fhorfheidhmiú
- > Caighdeán an uisce óil phoiblí agus phríobháidigh a mheasúnú agus tuairisciú air;
- > Comhordú a dhéanamh ar líonra d'eagraíochtaí seirbhíse poiblí chun tacú le gníomhú i gcoinne coireachta comhshaoil;
- > An dlí a chur orthu siúd a bhriseann dlí an chomhshaoil agus a dhéanann dochar don chomhshaol.

Bainistíocht Dramhaíola agus Ceimiceáin sa Chomhshaol

- > Rialacháin dramhaíola a chur i bhfeidhm agus a fhorfheidhmiú lena n-áirítear saincheisteanna forfheidhmithe náisiúnta;
- > Staitisticí dramhaíola náisiúnta a ullmhú agus a fhoilsiú chomh maith leis an bPlean Náisiúnta um Bainistíocht Dramhaíola Guaisí;
- > An Clár Náisiúnta um Chosc Dramhaíola a fhorbairt agus a chur i bhfeidhm;
- > Reachtaíocht ar rialú ceimiceán sa timpeallacht a chur i bhfeidhm agus tuairisciú ar an reachtaíocht sin.

Bainistíocht Uisce

- > Plé le struchtúir náisiúnta agus réigiúnacha rialachais agus oibriúcháin chun an Chreat-treoir Uisce a chur i bhfeidhm;
- > Monatóireacht, measúnú agus tuairisciú a dhéanamh ar chaighdeán aibhneacha, lochanna, uiscí idirchreasa agus cósta, uiscí snámha agus screamhuisce chomh maith le tomhas ar leibhéil uisce agus sreabhadh abhann.

Eolaíocht Aeráide & Athrú Aeráide

- > Fardail agus réamh-mheastacháin a fhoilsiú um astaíochtaí gás ceaptha teasa na hÉireann;
- > Rúnaíocht a chur ar fáil don Chomhairle Chomhairleach ar Athrú Aeráide agus tacaíocht a thabhairt don Idirphlé Náisiúnta ar Gníomhú ar son na hAeráide;

- > Tacú le gníomhaíochtaí forbartha Náisiúnta, AE agus NA um Eolaíocht agus Beartas Aeráide.

Monatóireacht & Measúnú ar an gComhshaol

- > Córais náisiúnta um monatóireacht an chomhshaoil a cheapadh agus a chur i bhfeidhm: teicneolaíocht, bainistíocht sonraí, anailís agus réamhaisnéisiú;
- > Tuairiscí ar Staid Thimpeallacht na hÉireann agus ar Tháscairí a chur ar fáil;
- > Monatóireacht a dhéanamh ar chaighdeán an aeir agus Treoir an AE i leith Aeir Ghlain don Eoraip a chur i bhfeidhm chomh maith leis an gCoinbhinsiún ar Aerthruailliú Fadraoin Trasteorann, agus an Treoir i leith na Teorann Náisiúnta Astaíochtaí;
- > Maoirseacht a dhéanamh ar chur i bhfeidhm na Treorach i leith Torainn Timpeallachta;
- > Measúnú a dhéanamh ar thionchar pleananna agus clár beartaithe ar chomhshaol na hÉireann.

Taighde agus Forbairt Comhshaoil

- > Comhordú a dhéanamh ar ghníomhaíochtaí taighde comhshaoil agus iad a mhaoiniú chun brú a aithint, bonn eolais a chur faoin mbeartas agus réitigh a chur ar fáil;
- > Comhoibriú le gníomhaíocht náisiúnta agus AE um thaighde comhshaoil.

Cosaint Raideolaíoch

- > Monatóireacht a dhéanamh ar leibhéil radaíochta agus nochtadh an phobail do radaíocht ianúcháin agus do réimsí leictreamaighnéadacha a mheas;
- > Cabhrú le pleananna náisiúnta a fhorbairt le haghaidh éigeandálaí ag eascairt as tasmí núicléacha;
- > Monatóireacht a dhéanamh ar fhorbairtí thar lear a bhaineann le saoráidí núicléacha agus leis an tsábháilteacht raideolaíochta;
- > Sainseirbhísí um chosaint ar an radaíocht a sholáthar, nó maoirsiú a dhéanamh ar sholáthar na seirbhísí sin.

Treoir, Ardú Feasachta agus Faisnéis Inrochtana

- > Tuairisciú, comhairle agus treoir neamhspleách, fianaise-bhunaithe a chur ar fáil don Rialtas, don tionscal agus don phobal ar ábhair maidir le cosaint comhshaoil agus raideolaíoch;
- > An nasc idir sláinte agus folláine, an geilleagar agus timpeallacht ghlan a chur chun cinn;
- > Feasacht comhshaoil a chur chun cinn lena n-áirítear tacú le hiompraíocht um éifeachtúlacht acmhainní agus aistriú aeráide;
- > Tástáil radóin a chur chun cinn i dtithe agus in ionaid oibre agus feabhsúchán a mholadh áit is gá.

Comhpháirtíocht agus Líonrú

- > Oibriú le gníomhaireachtaí idirnáisiúnta agus náisiúnta, údaráis réigiúnacha agus áitiúla, eagraíochtaí neamhrialtais, comhlachtaí ionadaíocha agus ranna rialtais chun cosaint comhshaoil agus raideolaíoch a chur ar fáil, chomh maith le taighde, comhordú agus cinnteoireacht bunaithe ar an eolaíocht.

Bainistíocht agus struchtúr na Gníomhaireachta um Chaomhnú Comhshaoil

Tá an GCC á bainistiú ag Bord lánaimseartha, ar a bhfuil Ard-Stiúrthóir agus cúigear Stiúrthóir. Déantar an obair ar fud cúig cinn d'Oifigí:

1. An Oifig um Inbhuanaitheacht i leith Cúrsaí Comhshaoil
2. An Oifig Forfheidhmithe i leith Cúrsaí Comhshaoil
3. An Oifig um Fhianaise agus Measúnú
4. An Oifig um Chosaint ar Radaíocht agus Monatóireacht Comhshaoil
5. An Oifig Cumarsáide agus Seirbhísí Corparáideacha

Tugann coistí comhairleacha cabhair don Ghníomhaireacht agus tagann siad le chéile go rialta le plé a dhéanamh ar ábhair imní agus le comhairle a chur ar an mBord.

EPA Research

Webpages: www.epa.ie/our-services/research/

LinkedIn: www.linkedin.com/showcase/eparesearch/

Twitter: @EPAResearchNews

Email: research@epa.ie

www.epa.ie